Classification: PHYSICAL SCIENCES – Sustainability Science

Climate related sea-level variations over the past two millennia

Andrew C. Kemp[1,2], Benjamin P. Horton[2*], Jeffrey P. Donnelly[3], Michael E. Mann[4], Martin Vermeer[5], Stefan Rahmstorf[6]

[1] School of Forestry and Environmental Studies and Yale Climate and Energy Institute, Yale University, New Haven, CT 06511, USA.

[2] Sea Level Research, Department of Earth and Environmental Science, University of Pennsylvania, Philadelphia, PA 19104, USA.

[3] Department of Geology and Geophysics, Woods Hole Oceanographic Institution, Woods Hole, MA 02543, USA.

[4] Department of Meteorology, Pennsylvania State University, University Park, PA 16802, USA.

[5] Department of Surveying, Aalto University School of Engineering, P.O. Box 11000, FI-00076 Aalto, Finland.

[6] Potsdam Institute for Climate Impact Research, Telegrafenberg A62, 14473 Potsdam, Germany.

*Corresponding author; bphorton@sas.upenn.edu, Tel: 215 573 5388, Fax: 215 898 5724

Abstract

We present new sea-level reconstructions for the past 2100 years based on salt-marsh sedimentary sequences from the US Atlantic coast. The data from North Carolina reveal four phases of persistent sea-level change after correction for glacial isostatic adjustment. Sea level was stable from at least BC 100 until AD 950. It then increased for 400 years at a rate of 0.6 mm/yr, followed by a further period of stable, or slightly falling, sea level that persisted until the late 19th century. Since then, sea level has risen at an average rate of 2.1 mm/yr, representing the steepest, century-scale increase of the past two millennia. This rate was initiated between AD 1865 and 1892. Using an extended semi-empirical modeling approach, we show that these sea-level changes are consistent with global temperature for at least the past millennium.

/body

Introduction

Climate and sea-level reconstructions encompassing the past 2000 years provide a pre-anthropogenic context for understanding the nature and causes of current and future changes. Hemispheric and global mean temperature have been reconstructed using instrumental records supplemented with proxy data from natural climate archives (1, 2). This research has improved understanding of natural climate variability and suggests that modern warming is unprecedented in the past two millennia (1). In contrast, understanding of sea-level variability during this period is limited and the response to known climate deviations such as the Medieval Climate Anomaly, Little Ice Age and 20th century warming is unknown. We reconstruct sea-level change over the past 2100 years using new salt-marsh proxy records and investigate the consistency of reconstructed sea level with global temperature using a semi-empirical relationship that connects sea-level changes to mean surface temperature (3, 4). The new sea-level proxy data constrain a multi-centennial response term in the semi-empirical model.

Results and Discussion

Sea-level data

Salt-marsh sediments and assemblages of foraminifera record former sea level because they are intrinsically linked to the frequency and duration of tidal inundation and keep pace with moderate rates of sea-level rise (5, 6). We developed transfer functions using a modern dataset of foraminifera (193 samples) from 10 salt marshes in North Carolina, USA (7). Transfer functions are empirically-derived equations for quantitatively

estimating past environmental conditions from paleontological data (8). The transfer functions were applied to foraminiferal assemblages preserved in 1 cm thick samples from two cores of salt-marsh sediment (Sand Point and Tump Point, North Carolina; Figure 1) to estimate paleomarsh elevation (PME), which is the tidal elevation at which a sample formed with respect to its contemporary sea level (9). Unique vertical errors were calculated by the transfer functions for each PME estimate and were less than 0.1 m. Composite chronologies were developed using AMS ^{14}C (conventional, high-precision and bomb-spike), a pollen chrono-horizon (increased *Ambrosia* at AD 1720±20 years), ^{210}Pb inventory and a ^{137}Cs spike (AD 1963). A probabilistic age-depth model (10) incorporating all dating results was generated separately for each core (Figure 1) to reduce chronological uncertainty and provide downcore age estimates at 1 cm intervals with uncertainties that varied from ±1 to ±71 years for 95% of samples.

Relative sea level (RSL) was reconstructed by subtracting transfer-function derived estimates of PME from measured sample altitudes (Figure 2B). Agreement of geological records with trends in regional and global tide-gauge data (Figures 2B and 3) validates the salt-marsh proxy approach and justifies its application to older sediments (11, 12). Despite differences in accumulation history and being more than 100 km apart, Sand Point and Tump Point recorded near identical RSL variations. This agreement suggests that local-scale factors including tidal-range change and sediment compaction were not important influences on RSL in the region over the past two millennia. Accord between the age and altitude of basal and non-basal samples (13, 14) provided further evidence that both records were free of detectable compaction.

To extract climate-related rates of sea-level rise (Figure 2C), we applied corrections for crustal movements associated with spatially variable and ongoing glacial isostatic adjustment (GIA). A constant rate of subsidence (with no error) was subtracted from the Sand Point (1.0 mm/yr) and Tump Point (0.9 mm/yr) records. These rates were estimated from a US Atlantic coast database of late Holocene (last 2000 years) sea-level index points (13, 15). Use of a constant rate is appropriate for this time period given Earth's rate of visco-elastic response (14). The resulting records are termed 'GIA adjusted', expressed relative to mean sea level from AD 1400-1800 and visually summarized by an envelope (Figure 2C). Using Bayesian multiple change-point regression (16), we identified four intervals (successive linear trends) of long-term (century scale), persistent sea-level variations with 95% confidence (Figure 2C). Within the error bounds of reconstructed sea level, greater variability in rates at sub-centennial time scales can be accommodated. From at least BC 100 until AD 950, sea level was stable (0.0 to +0.1 mm/yr). Between AD 850 and 1080 the rate of sea-level rise increased to 0.6 mm/yr (0.4 to 0.8 mm/yr) for the following 400 years. A second change point at AD 1270-1480 marked a return to stable, or slightly negative, sea level (-0.2 to 0.0 mm/yr), which persisted until the end of the 19th century. Between AD 1865 and 1892 sea-level rise increased to a mean rate of 2.1 mm/yr (1.9 to 2.2 mm/yr) (12). Sea-level variations in the last 2100 years did not exceed ±0.25 m until the onset of the modern rise in the late 19th century. The modern rate of sea-level rise was greater than any century-scale trend in the preceding 2100 years; a conclusion that is independent of the GIA correction applied.

Comparison with other proxy sea-level reconstructions

Most RSL reconstructions spanning the last 2000 years are from near- and intermediate-field regions affected by glacio-isostatic land movement because of their proximity to former ice sheets. To facilitate comparison among records, all sea-level reconstructions (including far-field regions) were adjusted for estimated GIA (Figure 3). In Massachusetts, we developed a new high-resolution reconstruction of RSL for the past 1500 years using macrofossils of common salt-marsh plants as sea-level indicators (Figure S1). Sea-level was stable prior to AD 500 and rose from AD 500 to 1000. The Massachusetts data agree with the North Carolina reconstruction, except for higher sea level between AD 700 and 1000 (although the uncertainty ranges overlap). There is a scarcity of high-resolution sea-level data covering the Medieval Climate Anomaly, particularly outside of North America (Figure 3). Salt-marsh proxy records from the Gulf of Mexico (17, 18) show stable sea level until AD 1000, followed by rise to a peak at AD 1200. In Connecticut, sea-level rose rapidly at AD 1000 (19), although this record maybe compromised by sedimentary hiatuses from hurricane erosion (20, 21). In Iceland, sea level fell gradually from AD 500 to 1800, possibly as a result of regional steric influences (22). All records from the Atlantic coast of North America, Gulf of Mexico and New Zealand (23) show stable or falling sea level between AD 1400 and 1900 at the time of the Little Ice Age. A record from Connecticut (6) developed using salt-marsh plant macrofossils showed stable sea level between AD 1300 and 1800 (Figure 3). The record from Maine (24) is inconclusive due to large uncertainties. In the Mediterranean Sea, archaeological evidence from Roman fish ponds in Italy located sea level 2000 years ago (50 BC to AD 100) at 0.13 m below present (25). In Israel, archaeological evidence

compiled from coastal wells showed falling or stable sea level between AD 100 and 900 (26), including sea level above present from AD 300 to 700. There is some evidence for a 1 m sea-level oscillation at AD 1000. In the Cook Islands (far-field region), reconstructions from coral microatolls proposed falling sea level over the last 2000 years, including two low stands in the last 400 years separated by a high stand at AD 1750 indicating sea-level oscillations of up to 0.6 m (27), that are not observed in other proxy records. Atlantic reconstructions constrain the onset of modern sea-level rise to AD 1880-1920 (12) and are supported by salt-marsh records from Spain (28-30) and New Zealand (23). The Icelandic record suggests that local sea-level rise began earlier (AD 1800-1840). There are no reconstructions spanning the transition to modern rates of sea-level rise from the Mediterranean or far-field and these sea-level proxies have not been validated against instrumental records.

Representation of global sea-level changes

There is close agreement between reconstructed sea level in North Carolina and compilations of global tide-gauge data (31, 32) (Figure 3; SI). Between AD 1700 and 1900, global sea level rose by 9±5 cm (32). Reconstructed sea-level rise in North Carolina for this period was 5±5 cm. GIA-adjusted RSL change from AD 1900 to 2000 in North Carolina (24±5 cm) exceeded the IPCC AR4 estimate for global 20th century rise (17±5 cm), although the uncertainty ranges overlap. Tide gauge estimates for 20th century sea-level rise were 16 cm (31) and 19 cm (32), but showed variability in rates of sea-level rise among ocean basins and confirm that 20th century rates in the northwest Atlantic exceeded the global average (33, 34). Regional deviations from global sea-level trends on

the time scales of interest arise from unforced variability around the mean and forced differences in regional trends. The former arise from natural climate modes such as ENSO. Differences in trend can be large over short time scales, but become progressively smaller as longer time scales are considered. Forced differences may arise from ocean circulation changes (35) in response to climate change (associated with regional temperature and salinity changes) and/or changes in gravitational field due to melting of continental ice sheets. In contrast to unforced oscillations, these forced deviations can increase in one direction as climate changes. Multi-centennial differences among regions are limited in magnitude by the restorative force of gravity, which pulls sea level toward the geoid. For North Carolina, we estimate that the deviation in sea-level rise from the global mean due to ocean circulation changes is between 0 and +5 cm. This estimate was based on the IPCC AR4 model ensemble for a 21st century global warming of ~3ºC, in which sea level rises globally by 22-48 cm. We take this as an upper limit estimate as temperature and sea-level variations over the last 2100 years were smaller (Figure 2A). The gravitational effect from continental ice sheet melting on sea level along the Atlantic coast is negative and we conclude that an upper limit is -5 cm for the largest sea-level variations in North Carolina (SI).

IPCC AR4 (Vol. 1 Figure 5.16) showed that local sea-level trends differed by up to 2 mm/yr from the global mean over AD 1955-2003, which implies deviations of up to ±10 cm at some locations (but ±5 cm along most coastlines) as the sum of forced and unforced effects. This analysis suggests that our data can be expected to track global

mean sea level within about ±10 cm over the past two millennia, within the uncertainty band shown for our analysis (Figure 2C).

Modeling sea level from global temperature on a millennial timescale

Based on physical considerations, Rahmstorf (3) proposed a proportionality between the rate global sea-level change H and global temperature T (as a deviation from a pre-industrial equilibrium T_0):

$$dH/dt = a\,(T-T_0) \qquad (1)$$

as a first-order approximation on time scales from a few decades to a few centuries. Semi-empirical models must be calibrated with data from the past (observational or proxy-based) to constrain how sea-level rise responded to temperature change. Applying this formula to the temperature record shown in Figure 2A yielded (after time integration) the blue sea-level curve in figure 4D. Here a=3.4 mm/yr/K was used as reported in (3) from observational data since AD 1880, but the pre-industrial temperature (which is not constrained well by these data) was adjusted within its uncertainty to -0.35 K (from -0.5 K, relative to mean temperature AD 1951-1980). With the extended formula and parameters of (4) similar results are obtained (using T_0=-0.35 K, instead of -0.41 K). The key difference is a larger acceleration factor (a=0.56) from correction for water stored in artificial reservoirs, which increases the climate-related component of 20th century sea-level rise. These two models (3, 4) were designed to describe only the short-term response, but are in good agreement with reconstructed sea level for the past 700 years.

The long proxy sea-level reconstruction from North Carolina gives a more robust constraint on the warming-induced, modern acceleration of sea-level rise (specifically by tight constraint of T_0), because it is sufficiently long to include a multi-century period of stable sea level (AD 1400-1880; Figure 2). It also provides an opportunity to improve on earlier semi-empirical studies by explicitly resolving the finite response time scale (τ) discussed (but then neglected due to the short time scale considered) in (3) and later implemented in (36).

Using the North Carolina data we thus added a term to the semi-empirical model of (3) as follows:

$$dH/dt = a_1[T(t) - T_{0,0}] + a_2[T(t) - T_0(t)] + b\, dT/dt \qquad (2a)$$

$$\text{with } dT_0/dt = \tau^{-1}[T(t) - T_0(t)] \qquad (2b)$$

The first term captures a slow response compared to the time scale of interest (now one or two millennia, rather than one or two centuries as in Eq. 1). The second term represents intermediate time scales, where an initial linear rise gradually saturates with time scale τ as base temperature (T_0) catches up with T. In Eq. 1, T_0 was assumed to be constant. The third term is the immediate response term introduced by (4); it is of little consequence for the slower sea-level changes considered in this paper.

Grinsted et al. (36) used a single term with time scale τ to model sea level. We retained the short- and very long-term components to describe the full sea-level response on all time scales. In the following analysis, we kept the constraints established from instrumental sea-level data for AD 1880-2000 (4), which control the rapid response term (parameter *b*) and the sum of the first two terms on the RHS of Eq. 2. Compatibility with values for AD 1880-2000 implies that the parameters in Eq. 1 and 2 are linked as follows to give the same total sea-level rise for this period from both equations:

$$a = a_1 + a_2 \text{ and } T_0 = (a_1 T_{0,0} + a_2 \langle T_0 \rangle)/a \qquad (3)$$

where $\langle T_0 \rangle$ is the average of $T_0(t)$ over AD 1880-2000. If the resulting time scale τ in Eq. 2 is multi-century, $T_0(t)$ will vary little and sea-level curves for AD 1880-2000 will be almost identical to those shown in (4). The parameter values found previously (3) for this time period were:

$$a = 0.56 \pm 0.05 \text{ cm/a/K}; \; b = -4.9 \pm 1.0 \text{ cm/K}; \text{ and } T_0 = -0.41 \pm 0.03 \text{ K}. \qquad (4)$$

Hence two new parameters, a_2 and τ, together with an initial value $T_{0,0}$, are introduced, which need to be constrained from the new sea-level reconstruction. To do so, we forced the model with a global temperature record, $T(t)$, for AD 500-1850 (1). The two parameters were then constrained through Monte-Carlo simulations combined with Bayesian updating from the North Carolina sea-level reconstruction (36).

A priori solution

We generated temperature curves using the Mann et al. (1) reconstruction (global land and ocean, Error-in-Variables, EIV) and its formal uncertainties (Table S3). These data fulfilled our requirement of global (not just hemispheric) land and ocean coverage. For the instrumental period (temperatures based on HADCrutv3), we conservatively assumed error margins of ±0.06 K for AD 1850-1950 and ±0.04 K for AD 1950-2006 for decadal averages. These formed an uncertainty band surrounding the Mann et al. (1) temperature curve (Figure 4A). Temperature curves were translated into corresponding sea-level curves using Eqs. 2 and 3. We described the prior uncertainties of the fit parameters a_1, a_2, b, $T_{0,0}$, $T_0(t)$ and τ. For a, b and $\langle T_0 \rangle$ we took the values given in Eq. 4 as true. Our *a priori* error distributions are presented in table S3.

An ensemble of sea-level curves, $T_0(t)$, and its uncertainties were computed by integrating Eq. (2). Figure 4B shows the *a priori* analysis with all parameters varied across their full *a priori* uncertainty ranges. Since AD 1000, reconstructed sea level from North Carolina was within the uncertainty bands for sea level predicted from the paleo-temperature data of Mann et al. (1), showing broad consistency among proxy sea level and proxy temperature data under the semi-empirical relationship (Eq. 2).

A posteriori solution

We combined the two sources of data to constrain parameters and narrow uncertainty by using the North Carolina sea-level data to perform a Bayesian update on the *a priori* solution (SI). After constraining the parameters of the semi-empirical model (Figure 5), a good agreement among predicted and reconstructed sea levels was achieved (Figure 4D).

Predicted sea level also agreed well with instrumental (tide gauge) data (31) since AD 1880 (Figure 6).

To find acceptable agreement, τ must be finite and probably less than 1000 years (Figure S3). This result is robust against inflating the uncertainties of Eq. 4 by a factor of 10, showing it to hold for a broad range of semi-empirical fit parameters, not just those derived in (4). See SI for details.

Divergence arises before AD 1000, when predicted sea level leaves the 2σ uncertainty band of reconstructed sea level, including GIA uncertainty of ±0.15mm/yr (Figure 4). Reconstructed temperature showed warmer temperatures before AD 1000 compared to after, while reconstructed sea level was stable before AD 1000, but rose thereafter (AD 1000-1400). This is fundamentally inconsistent with warmer global temperatures causing sea level to rise. A possible explanation is that reconstructed global temperature (1) was systematically high prior to AD 1000. Northern Hemisphere temperature reconstructions are generally cooler than the global average for this period (2). Lowering global temperature by 0.2 K over the period AD 500-1100 removes this discrepancy. This illustrates how tightly input temperatures constrain sea level computed by the semi-empirical model, making the good agreement for the past millennium all the more significant.

Conclusions

We have presented a new, high-resolution sea-level reconstruction developed using salt-marsh sediments for the last 2100 years from the US Atlantic coast. Post-AD 1000, these sea-level reconstructions are compatible with reconstructions of global temperature, assuming a linear relation between temperature and the rate of sea-level rise. This consistency mutually reinforces the credibility of the temperature and sea-level reconstructions. According to our analysis, North Carolina sea level was stable from BC 100 to AD 950. Sea-level rose at a rate of 0.6 mm/yr from about AD 950 to 1400 as a consequence of Medieval warmth, although there is a difference in timing when compared to other proxy sea-level records. North Carolina and other records show sea-level was stable from AD 1400 until the end of the 19th century due to cooler temperatures associated with the Little Ice Age. A second increase in the rate of sea-level rise occurred around AD 1880-1920; in North Carolina the mean rate of rise was 2.1 mm/yr in response to 20th century warming. This historical rate of rise was greater than any other persistent, century-scale trend during the past 2100 years.

Materials and Methods

Sea level in North Carolina was reconstructed using transfer functions relating the distribution of salt-marsh foraminifera to tidal elevation (7, 12). Application of transfer functions to samples from two cores (at sites 120 km apart) of salt-marsh sediment provided estimates of PME with uncertainties of <0.1 m. For each core a probabilistic age-depth model (10) was developed from composite chronological results and allowed the age of any sample to be estimated with 95% confidence . In Massachusetts, plant

macrofossils preserved in salt-marsh sediment overlying a glacial erratic, were dated using AMS ^{14}C and pollen and pollution chronohorizons (Figure S1). The modern distribution of common salt-marsh plants was used to estimate PME. Sea level was reconstructed by subtracting estimated PME from measured sample altitude. Corrections for GIA were estimated from local (13) and US Atlantic coast (15) databases of late Holocene sea-level index points. Detailed methods are presented in SI text.

Acknowledgments

Research was supported by NSF grants (EAR-0951686) to BPH and JPD. ACK thanks a NOSAMS internship, UPenn paleontology stipend and grants from GSA and NAMS. North Carolina sea-level research was funded by NOAA (NA05NOS4781182), USGS (02ERAG0044) and NSF (EAR-0717364) grants to BPH with S. Culver and R. Corbett (East Carolina University). JPD (EAR-0309129) and MEM (ATM-0542356) acknowledge NSF support. MV acknowledges Academy of Finland Project 123113 and COST Action ES0701. Dana MacDonald counted Wood Island pollen. R. Gehrels provided the Nova Scotia sea-level data. We thank L. Neureither (Potsdam Institute for Climate Impact Research) for critically reviewing the modeling code and algorithm description and A. Parnell (University College Dublin) for statistical support. D. Hill (Oregon State University) and J. Feyen (NOAA) performed tidal modeling.

References

1. Mann ME, *et al.* (2008) Proxy-based reconstructions of hemispheric and global surface temperature variations over the past two millennia. *Proceedings of the National Academy of Sciences* 105(36):13252-13257.
2. Jansen E, *et al.* (2007) Paleoclimate. *Climate Change 2007: The Physical Science Basis. Contribution of Working Group I to the Fourth Assessment Report of the Intergovernmental Panel on Climate Change*, eds Solomon S, Qin D, Manning M, Chen Z, Marquis M, Averyt KB, Tignor M, & Miller HL (Cambridge University Press, New York City).
3. Rahmstorf S (2007) A Semi-Empirical Approach to Projecting Future Sea-Level Rise. *Science* 315(5810):368-370.
4. Vermeer M & Rahmstorf S (2009) Global sea level linked to global temperature. *Proceedings of the National Academy of Sciences* 106(51):21527-21532.
5. Horton B & Edwards R (2006) *Quantifying Holocene sea-level change using intertidal foraminifera: lessons from the British Isles* p 97.
6. Donnelly JP, Cleary P, Newby P, & Ettinger R (2004) Coupling instrumental and geological records of sea-level change: evidence from southern New England of an increase in the rate of sea-level rise in the late 19th century. *Geophysical Research Letters* 31(5):L05203.
7. Kemp AC, Horton BP, & Culver SJ (2009) Distribution of modern salt-marsh foraminifera in the Albemarle-Pamlico estuarine system of North Carolina, USA: Implications for sea-level research. *Marine Micropaleontology* 72(3-4):222-238.
8. Sachs HM, Webb T, & Clark DR (1977) Paleoecological Transfer Functions. *Annual Review of Earth and Planetary Sciences* 5(1):159-178.
9. Edwards RJ (2007) Sea Level Studies: Low energy coasts sedimentary indicators. *Encyclopedia of Quaternary Science*, ed Elias SA (Elsevier, Amsterdam), pp 2994-3005.
10. Parnell AC, Haslett J, Allen JRM, Buck CE, & Huntley B (2008) A flexible approach to assessing synchroneity of past events using Bayesian reconstructions of sedimentation history. *Quaternary Science Reviews* 27(19-20):1872-1885.
11. Gehrels WR, *et al.* (2005) Onset of recent rapid sea-level rise in the western Atlantic Ocean. *Quaternary Science Reviews* 24(18-19):2083-2100.
12. Kemp AC, *et al.* (2009) Timing and magnitude of recent accelerated sea-level rise (North Carolina, United States). *Geology* 37(11):1035-1038.
13. Horton BP, *et al.* (2009) Holocene sea-level changes along the North Carolina Coastline and their implications for glacial isostatic adjustment models. *Quaternary Science Reviews* 28(17-18):1725-1736.
14. Peltier WR (2001) Global sea level rise and glacial isostatic adjustment: an analysis of data from the east coast of North America. *Geophysical Research Letters* 23.
15. Engelhart SE, Horton BP, Douglas BC, Peltier WR, & Tornqvist TE (2009) Spatial variability of late Holocene and 20th century sea-level rise along the Atlantic coast of the United States. *Geology* 37(12):1115-1118.
16. Carlin BP, Gelfand AE, & Smith AFM (1992) Hierarchical Bayesian Analysis of Changepoint Problems. *Applied Statistics* 41(2):389-405.

17. Tornqvist TE, Bick SJ, van der Borg K, & de Jong AFM (2006) How stable is the Mississippi Delta? *Geology* 34(8):697-700.
18. González JL & Törnqvist TE (2009) A new Late Holocene sea-level record from the Mississippi Delta: evidence for a climate/sea level connection? *Quaternary Science Reviews* 28(17-18):1737-1749.
19. van de Plassche O, van der Borg K, & de Jong AFM (1998) Sea level-climate correlation during the past 1400 yr. *Geology* 26(4):319-322.
20. van de Plassche O, *et al.* (2006) Salt-marsh erosion associated with hurricane landfall in southern New England in the fifteenth and seventeenth centuries. *Geology* 34(10):829-832.
21. van de Plassche O, Wright AJ, van der Borg K, & de Jong AFM (2004) On the erosive trail of a 14th and 15th century hurricane in Connecticut (USA) salt marshes. *Radiocarbon* 46(2):775-784.
22. Gehrels WR, *et al.* (2006) Rapid sea-level rise in the North Atlantic Ocean since the first half of the nineteenth century. *Holocene* 16(7):949-965.
23. Gehrels WR, Hayward B, Newnham RM, & Southall KE (2008) A 20th century acceleration of sea-level rise in New Zealand. *Geophysical Research Letters* 35(2):L02717.
24. Gehrels WR, Belknap DF, Black S, & Newnham RM (2002) Rapid sea-level rise in the Gulf of Maine, USA, since AD 1800. *The Holocene* 12(4):383-389.
25. Lambeck K, Anzidei M, Antonioli F, Benini A, & Esposito A (2004) Sea level in Roman time in the Central Mediterranean and implications for recent change. *Earth and Planetary Science Letters* 224(3-4):563-575.
26. Sivan D, *et al.* (2004) Ancient coastal wells of Caesarea Maritima, Israel, an indicator for relative sea level changes during the last 2000 years. *Earth and Planetary Science Letters* 222(1):315-330.
27. Goodwin ID & Harvey N (2008) Subtropical sea-level history from coral microatolls in the Southern Cook Islands, since 300 AD. *Marine Geology* 253(1-2):14-25.
28. Garcia-Artola A, Cearreta A, Leorri E, Irabien MJ, & Blake WH (2009) Coastal salt-marshes as geological archives of recent sea-level changes. (Translated from Spanish) *Geogaceta* 47:109-112 (in Spanish).
29. Leorri E, Cearreta A, & Horton BP (2008) A foraminifera-based transfer function as a tool for sea-level reconstructions in the southern Bay of Biscay. *Geobios* 41(6):787-797.
30. Leorri E, Horton BP, & Cearreta A (2008) Development of a foraminifera-based transfer function in the Basque marshes, N. Spain: Implications for sea-level studies in the Bay of Biscay. *Marine Geology* 251(1-2):60-74.
31. Church JA & White NJ (2006) A 20th century acceleration in global sea-level rise. *Geophysical Research Letters* 33(1):L01602.
32. Jevrejeva S, Moore JC, Grinsted A, & Woodworth PL (2008) Recent global sea level acceleration started over 200 years ago? *Geophysical Research Letters* 35(8):L08715.
33. Jevrejeva S, Grinsted A, Moore JC, & Holgate S (2006) Nonlinear trends and multiyear cycles in sea level records. *Journal of Geophysical Research* 111(C9):C09012.

34. Woodworth PL, *et al.* (2009) Evidence for the accelerations of sea level on multi-decade and century timescales. *International Journal of Climatology* 29(6):777-789.
35. Yin J, Schlesinger ME, & Stouffer RJ (2009) Model projections of rapid sea-level rise on the northeast coast of the United States. *Nature Geoscience* 2(4):262-266.
36. Grinsted A, Moore J, & Jevrejeva S (2009) Reconstructing sea level from paleo and projected temperatures 200 to 2100 ad. *Climate Dynamics*:doi: 10.1007/s00382-00008-00507-00382.

Figure Legends

Figure 1: Litho-, bio- and chronostratigraphy of the Sand Point (**A**) and Tump Point (**B**) cores (North Carolina, USA). Chronologies were developed using Accelerator Mass Spectrometry (AMS) ^{14}C dating (conventional, high-precision, HP, and bombspike), ^{210}Pb, ^{137}Cs and a pollen horizon. All dating results were combined to produce a probabilistic age-depth model for each core (10), shown as a grey-shaded area (95% confidence limits). This model estimated the age (with unique uncertainty) of samples at 1 cm resolution. Paleo marsh elevation (PME) above mean sea level (MSL) was estimated for each sample by application of transfer functions to complete foraminiferal assemblages. Only the most abundant species are shown (Hm=*Haplophragmoides manilaensis*). Relative sea level (RSL) was estimated by subtracting PME from measured sample altitude.

Figure 2: (**A**) Composite Error-In-Variables (EIV) global land plus ocean global temperature reconstruction (1), smoothed with a 30-year LOESS low-pass filter (blue). Data since AD 1850 (red) are HADCrutv3 instrumental temperatures. Values are relative to a pre-industrial average for AD 1400-1800 (**B**) RSL reconstructions at Sand Point and Tump Point since BC 100. Boxes represent sample-specific age and sea-level uncertainties (2σ). Inset is a comparison with nearby tide-gauge data. (**C**) GIA-adjusted sea-level at Sand Point and Tump Point expressed relative to a pre-industrial average for AD 1400-1800. Sea-level data points are represented by parallelograms because of distortion caused by GIA, which has a larger effect on the older edge of a data point than on the younger edge. Times of changes in the rate of sea-level rise (95% confidence

change point intervals) are shown. Pink envelope is a 9 degree polynomial to visually summarize the North Carolina sea-level reconstruction.

Figure 3: Late Holocene sea-level reconstructions after correction for glacio-isostatic adjustment (GIA). The rate applied (listed in panels) was taken from the original publication when possible. In Israel, land and ocean basin subsidence had a net effect of zero (26). Reconstructions from salt marshes are shown in blue; archaeological data in green and coral microatolls in red. Tide-gauge data expressed relative to AD 1950-2000 average, error from (32) in grey. Vertical and horizontal scales for all datasets are the same, and are provided in the North Carolina panel. Datasets were vertically aligned for comparison with the summarized North Carolina reconstruction (pink).

Figure 4: *A priori* and *a posteriori* sea-level predicted from paleo-temperature data. Temperature and GIA-adjusted sea level are expressed relative to AD 1400-1800 averages. Shaded error bands indicate 1σ and 2σ uncertainties. (**A**) *A priori* temperature (grey) and equilibrium temperature (blue). (**B**) *A priori* sea level predicted from temperature (grey) and summary of North Carolina sea-level reconstruction as cutaway bands (pink). An additional, systematic, GIA uncertainty (additive linear trend of 0.15 mm/yr) is indicated by dashed red lines and exceeds the 2σ uncertainty of estimated GIA (0.1 mm/yr). Temperatures and model parameters are set to the *a priori* distributions (Table S3). (**C**) *A posteriori* temperature (grey, original from (1) is the red line) and equilibrium temperature $T_0(t)$ (blue). (**D**) Sea level predicted from temperature (grey) with summary of North Carolina sea-level reconstruction (pink). Salt-marsh proxy data

used in Bayesian update were down-weighted by a factor of 10 and used only after AD 1000. Sea-level predicted from (4) and (3) are shown for comparison. Dashed red lines are as panel B.

Figure 5: Posterior probability density distributions and correlation point clouds for unknown parameters and functions of interest; ka is thousands of years.

Figure 6: Comparison of posterior solution with instrumental (tide gauge) data for AD 1880-2000. Black, grey: predicted sea level based on Mann et al. (1) temperatures (effectively HADcrutv3), as shown in Figure 4D. Blue: Church and White (31) sea level, corrected for the artificial reservoir storage contribution (4).

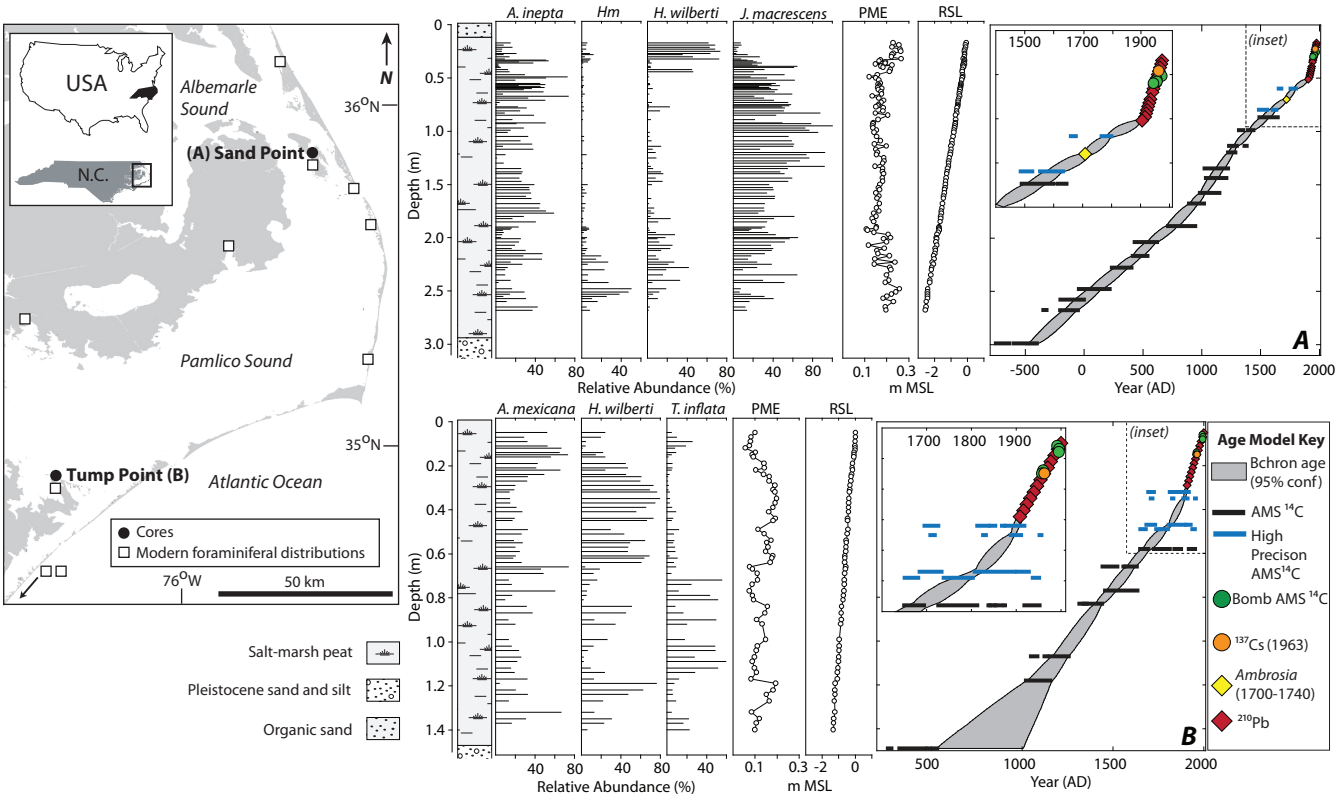
USA
N.C.
Albemarle Sound
(A) Sand Point
Pamlico Sound
Tump Point (B)
Atlantic Ocean
N
36°N
35°N
76°W
50 km
Cores
Modern foraminiferal distributions
Salt-marsh peat
Pleistocene sand and silt
Organic sand
A. inepta
Hm
H. wilberti
J. macrescens
PME
RSL
Depth (m)
Relative Abundance (%)
m MSL
Year (AD)
(inset)
A
A. mexicana
H. wilberti
T. inflata
PME
RSL
Relative Abundance (%)
m MSL
Year (AD)
(inset)
B
Age Model Key
Bchron age (95% conf)
AMS 14C
High Precison AMS14C
Bomb AMS 14C
137Cs (1963)
Ambrosia (1700-1740)
210Pb

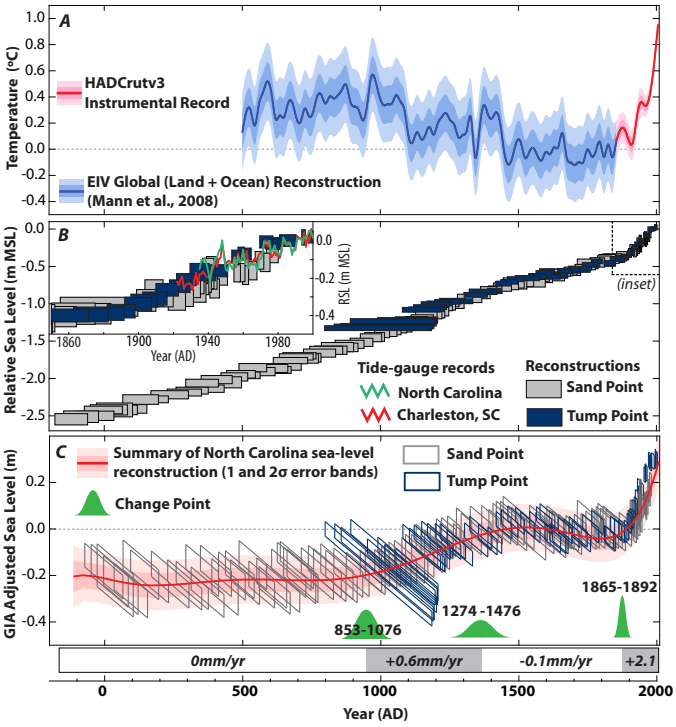
A
Temperature (°C)
HADCrutv3
Instrumental Record
EIV Global (Land + Ocean) Reconstruction
(Mann et al., 2008)
B
Relative Sea Level (m MSL)
RSL (m MSL)
Year (AD)
(inset)
Tide-gauge records
North Carolina
Charleston, SC
Reconstructions
Sand Point
Tump Point
C
GIA Adjusted Sea Level (m)
Summary of North Carolina sea-level
reconstruction (1 and 2σ error bands)
Change Point
Sand Point
Tump Point
1865-1892
1274 -1476
853-1076
0mm/yr
+0.6mm/yr
-0.1mm/yr
+2.1
Year (AD)

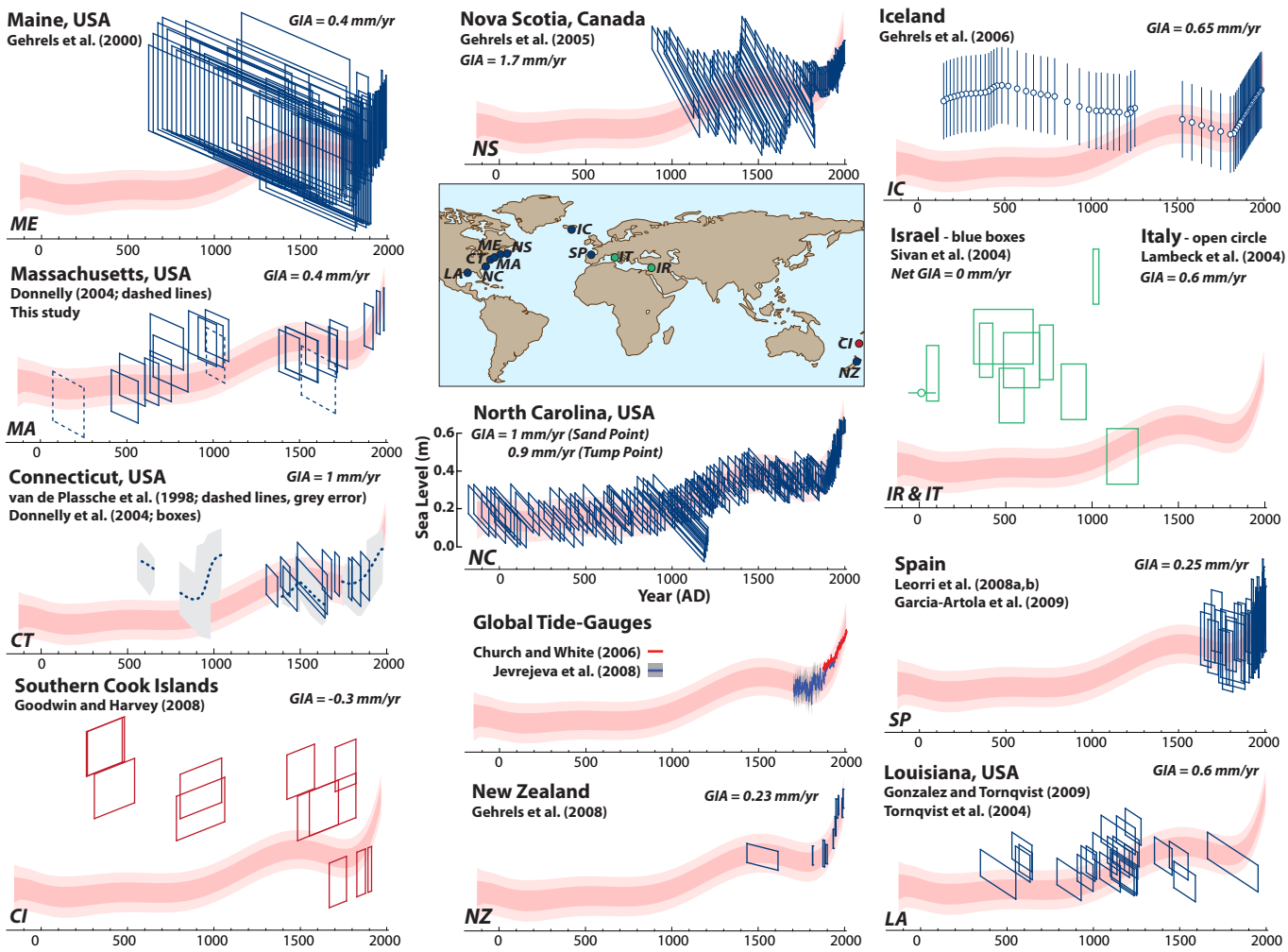
Maine, USA
Gehrels et al. (2000)
GIA = 0.4 mm/yr
ME
Massachusetts, USA
Donnelly (2004; dashed lines)
This study
GIA = 0.4 mm/yr
MA
Connecticut, USA
van de Plassche et al. (1998; dashed lines, grey error)
Donnelly et al. (2004; boxes)
GIA = 1 mm/yr
CT
Southern Cook Islands
Goodwin and Harvey (2008)
GIA = -0.3 mm/yr
CI
Nova Scotia, Canada
Gehrels et al. (2005)
GIA = 1.7 mm/yr
NS
IC
ME
NS
CT
MA
LA
NC
SP
IT
IR
CI
NZ
North Carolina, USA
GIA = 1 mm/yr (Sand Point)
0.9 mm/yr (Tump Point)
Sea Level (m)
0.6
0.4
0.2
0.0
NC
Year (AD)
Global Tide-Gauges
Church and White (2006)
Jevrejeva et al. (2008)
New Zealand
Gehrels et al. (2008)
GIA = 0.23 mm/yr
NZ
Iceland
Gehrels et al. (2006)
GIA = 0.65 mm/yr
IC
Israel - blue boxes
Sivan et al. (2004)
Net GIA = 0 mm/yr
Italy - open circle
Lambeck et al. (2004)
GIA = 0.6 mm/yr
IR & IT
Spain
Leorri et al. (2008a,b)
Garcia-Artola et al. (2009)
GIA = 0.25 mm/yr
SP
Louisiana, USA
Gonzalez and Tornqvist (2009)
Tornqvist et al. (2004)
GIA = 0.6 mm/yr
LA
0
500
1000
1500
2000

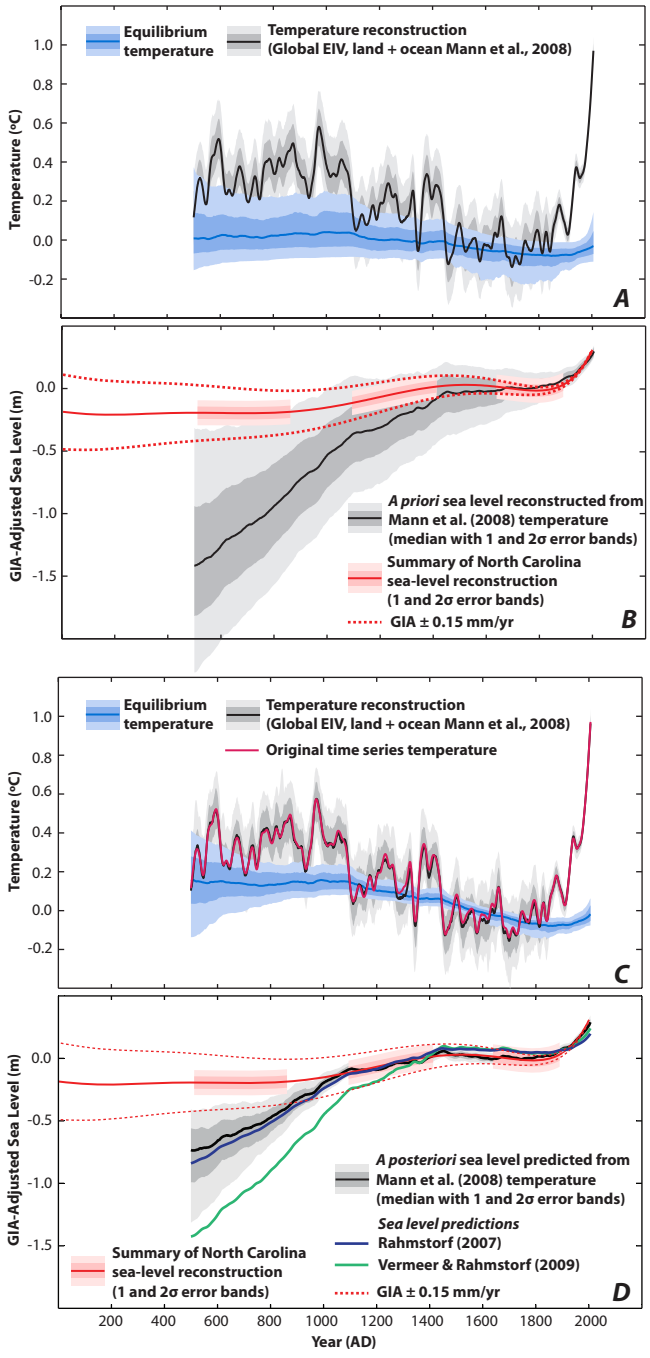
Equilibrium temperature
Temperature reconstruction (Global EIV, land + ocean Mann et al., 2008)
Temperature (°C)
1.0
0.8
0.6
0.4
0.2
0.0
-0.2
A
GIA-Adjusted Sea Level (m)
0.0
-0.5
-1.0
-1.5
A priori sea level reconstructed from Mann et al. (2008) temperature (median with 1 and 2σ error bands)
Summary of North Carolina sea-level reconstruction (1 and 2σ error bands)
GIA ± 0.15 mm/yr
B
Equilibrium temperature
Temperature reconstruction (Global EIV, land + ocean Mann et al., 2008)
Original time series temperature
Temperature (°C)
C
GIA-Adjusted Sea Level (m)
A posteriori sea level predicted from Mann et al. (2008) temperature (median with 1 and 2σ error bands)
Sea level predictions
Rahmstorf (2007)
Vermeer & Rahmstorf (2009)
GIA ± 0.15 mm/yr
Summary of North Carolina sea-level reconstruction (1 and 2σ error bands)
D
200
400
600
800
1000
1200
1400
1600
1800
2000
Year (AD)

Figure 5

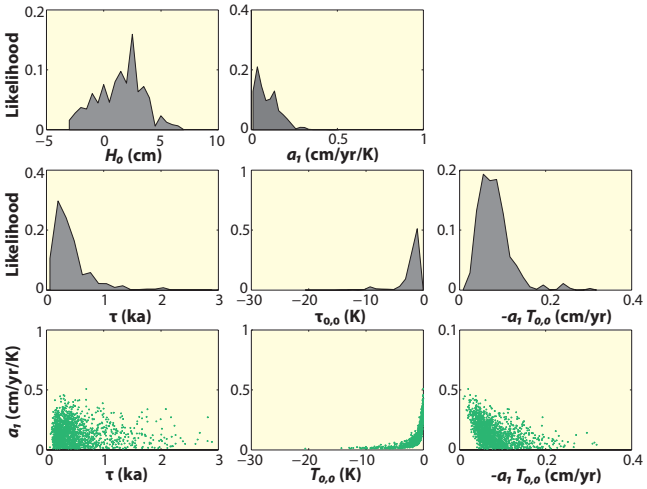
Likelihood
H_o (cm)
a_1 (cm/yr/K)
τ (ka)
$\tau_{o,o}$ (K)
$-a_1 T_{o,o}$ (cm/yr)
a_1 (cm/yr/K)
$T_{o,o}$ (K)

FIGURE 6

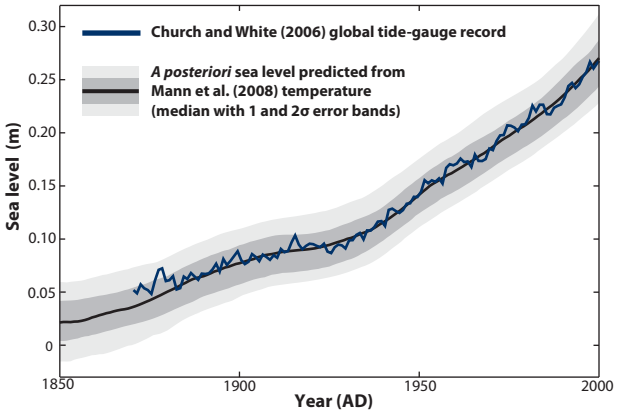
Church and White (2006) global tide-gauge record
A posteriori sea level predicted from Mann et al. (2008) temperature (median with 1 and 2σ error bands)
Sea level (m)
0.30
0.25
0.20
0.15
0.10
0.05
0
1850
1900
1950
2000
Year (AD)

Climate related sea-level variations over the past two millennia

Supporting Information

Reconstructing relative sea level in North Carolina and Massachusetts

In North Carolina, a modern dataset of 193 surface samples collected from 10 salt marshes (1) was used to develop transfer functions to quantify the relationship between foraminifera and elevation (2). We used these transfer functions to estimate paleomarsh elevation (PME) at Sand Point and Tump Point, North Carolina. PME is the elevation at which a sample formed with respect to its contemporary sea level (3). Foraminifera preserved in 1 cm thick samples from the Sand Point and Tump Point cores provided the basis for estimating PME. To reconstruct RSL, estimated PME was subtracted from the measured altitude of each sample. Core-top elevations were established by leveling to geodetic benchmarks (Sand Point) and Real Time Kinematic satellite navigation (Tump Point), thus sample altitude was derived from depth-in-core measurements. Foraminifera and PME estimates for the Sand Point and Tump Point cores are presented in Figure 1. Transfer functions provide error estimates that are unique to each sample (4). Uncertainty from sampling (e.g. angle of bore hole, sample thickness, RTK error) was minimal and not included in the vertical sea-level errors.

At Wood Island (Massachusetts), salt-marsh plants were used as sea-level indicators (5). The modern mean elevation of *Juncus geradii* (Jg), *Spartina patens* (Sp) and *Distichlis spicata* (Ds) was estimated by measuring stands at the Wood Island site. Multiple, stratigraphically ordered, samples were recovered along the boundary between a gently

sloping granite outcrop and overlying salt-marsh sediments. Identifiable remains of Jg, Sp and Ds were used to provide an estimate of PME (Figure S1).

Developing composite chronologies for North Carolina and Massachusetts

Original dating results for North Carolina and Massachusetts are provided in a separate file. A separate chronology was developed for the Sand Point and Tump Point cores, which were not combined or used to constrain one another in any way. The uppermost part of both cores was dated using a ^{210}Pb derived accumulation history. Sample ages were estimated using the constant supply constant flux model (6), which was independently corroborated by a ^{137}Cs peak (corresponding to AD 1963) and bomb-spike ^{14}C dates. Material prepared for bomb-spike ^{14}C dating was analyzed using Accelerator Mass Spectrometry (AMS) with 15 repeats of 30 000 counts. Multiple samples were dated to facilitate calibration using the Northern Hemisphere Zone 2 dataset of Reimer et al. (7). High-precision ^{14}C ages (8) were obtained by preparing duplicate or triplicate samples from the same depth interval and using a pooled mean (Calib 5.0.1) for calibration. Radiocarbon activity was determined from 15 repeats of 30,000 counts to improve instrument-related precision. Calibration was undertaken using Calib 5.0.1, reported errors are 2σ. An additional 15 samples at Sand Point and 7 at Tump Point were dated using conventional AMS ^{14}C. Calibration was undertaken using Calib 5.0.1, reported errors are 2σ. All samples were prepared for radiocarbon dating by cleaning under a binocular microscope to remove contaminating material. A pollen chrono-horizon was identified in the Sand Point core by an increase in *Ambrosia* to 2% of

total pollen, this change is indicative of land clearance during European settlement and was assigned an age of AD 1720 ± 20 years (9).

The discreet dated samples from Sand Point and Tump Point were used to generate a probabilistic age-depth model for each of the cores separately using the statistical package *Bchron* (10) executed in *R*. This approach used many thousands of iterations of the available data to provide an age-depth model with 95% confidence. This model was subsequently used to estimate the age (with a unique uncertainty) of every 1cm thick sample in both cores, including those that were not directly dated. The uncertainty associated with estimating the age of individual 1cm thick intervals ranged from ± 1 year (minimum) to ± 193 years (maximum), although more than 95% of samples had uncertainty of less than ± 71 years. In general, the smallest chronological errors were in the uppermost sections of each core (most recent), where age was constrained by techniques (^{210}Pb, ^{137}Cs, bomb-spike ^{14}C and a pollen chrono-horizon) with small error terms. The chronologies (dates and age-depth models) for the Sand Point and Tump Point cores are presented in Figure 1.

In Massachusetts, each of the samples used for estimating PME was also dated. 14 of the plant macrofossil samples were directly dated using AMS ^{14}C. Pollen evidence of European land clearance (AD 1700 in this region) and the chestnut decline (AD 1930) were used to estimate the age of two samples. A peak in ^{137}Cs associated with above ground testing of nuclear weapons was assigned an age of AD 1963 and an industrial horizon (AD 1875) was recognized by increased Pb and Cu concentrations and the

occurrence of opaque spherules. The stratigraphical relationship between samples was used manually to better constrain the chronology derived from calibrated ^{14}C ages and reduce uncertainty. The dates and age model for the Wood Island site are presented in figure S1. The elevation-depth model, developed using Bchron (10), supports the manual constraint of the chronology.

All sea-level data points are represented by boxes incorporating the elevational and chronological uncertainties associated with individual samples. This data is presented in Table S1 for North Carolina and for Massachusetts. Reconstructed sea level from the Sand Point and Tump Point cores for the last ~400 years was presented by Kemp et al. (2). However, the data presented here spanning the last 400 years improve upon the existing record by introducing additional foraminiferal counts and new, statistically rigorous age-depth models developed using a newer technique.

In the main manuscript the data points reconstructing sea level in North Carolina are summarized using a 9 degree polynomial with 1σ and 2σ errors used to create a sea-level envelope which we have presented in pink. The purpose of this envelope is solely to provide a convenient visual summary of the data to aid the reader. The polynomial summary was not used for analysis of sea-level change in North Carolina.

Estimating vertical land movements associated with glacial isostatic adjustment (GIA)

Reconstructions of relative sea level are the net result of eustatic, isostatic, tectonic and local factors. We assumed the tectonic factor to be zero in North Carolina and agreement between reconstructions from Sand Point and Tump Point (120 km apart) suggested that local factors were not a major influence. By assuming that the eustatic contribution to sea-level change over the last 2000 years was minimal (11), late Holocene sea-level reconstructions can be used to estimate the rate of GIA. A zero late Holocene sea-level eustatic function is a feature of most GIA models (12-14).

We used a standardized database of sea-level reconstructions collated for the US Atlantic coast to estimate the rate of GIA in North Carolina (15, 16). All data points that were not of base of basal or basal origin were excluded to negate the influence of sediment consolidation. Linear regression of the sea-level data points over the last 2000 years (excluding changes since AD 1900) estimated the rate of GIA to be 1.00 ± 0.03 mm/yr in the region of Sand Point and 0.90 ± 0.02 mm/yr at Tump Point. This uncertainty is the 2σ error of the regression line. Linear regression of mid-point sea-level reconstructions is appropriate for estimating rates of GIA in regions with sea-level histories constrained by a large number of data points with small age and vertical errors such as North Carolina (16). Model predictions support the use of a single linear rate of GIA over the late Holocene given Earth's rate of viscoelastic response (12-14). Predictions specifically for the areas around Sand Point and Tump Point show linear GIA for the last 2000 years (15). According to (16), there is 95% confidence that estimated rates of GIA (using this

method) over the last 4000 years in North Carolina were within 0.10 mm/yr of the values we have applied. GIA uncertainty has a propagating effect when used to adjust geological data because it becomes increasingly large further back in time. We did not include this effect as a stochastic error in our sea-level reconstruction (Figures 2 and 3), but visually illustrate its influence by conservatively assuming a a GIA uncertainty of ± 0.15 mm/yr in Figure 4.

Direct comparison among sea-level records is facilitated by correcting sea-level reconstructions for the effect of GIA. Uncertainty in estimating rates of GIA is therefore a possible cause for differences among records, the effect of which becomes increasingly large as reconstructions are extended farther back in time. All sites required correction for GIA. However, the location of a sea-level reconstruction (near, intermediate or far field) does not influence the uncertainty of estimated GIA only its absolute value. In fact, uncertainty is proportionally less at sites experiencing high rates of GIA. Regional estimates of GIA have been derived from geological data or model predictions. Uncertainty is therefore dependent upon the quality of available geological data or the accuracy of model predictions which themselves have often been calibrated using sea-level data. The US Atlantic coast has one of the most detailed records of late Holocene sea level and sufficient, quality controlled data exists to identify to identify regional GIA trends with confidence.

The rate of GIA for Wood Island and Revere, Massachusetts (0.4 mm/yr) and Barn Island (5), Connecticut (1 mm/yr) was estimated using the same approach as described for North

Carolina. In figure 3, all sea-level records presented have had estimated GIA removed. Other published studies of late Holocene sea-level change were adjusted for rates of glacio-isostatic adjustment (GIA) using estimates presented in the original publication (Maine (17), Nova Scotia (17, 18), Louisiana (19), Iceland (20), Israel (21)), Italy (22) and the Cook Islands (23)), or from (24) in the cases of Spain and New Zealand. No GIA correction was applied to the Israel data because the original publication states that the net effect was zero (21) because the rate of land subsidence was offset by ocean basin subsidence. In the Cook Islands, GIA is solely from subsidence of the ocean basin (23). In each example, except the record from Connecticut (25), sea-level data (and associated errors) were taken directly from the original publication or kindly provided by the author.

Estimating rates of sea-level change

Following adjustment for rates of GIA, we estimated rates of sea-level change for North Carolina. The datasets from Sand Point and Tump Point were only merged after this adjustment, by combining the age and sea-level estimates associated with individual data points into a single list. The sea-level data for North Carolina is complex because it consists of a large number of data points that are not spaced at regular temporal intervals and each of which has unique vertical and age uncertainties with an associated error distribution. Given the nature of the data, we used Bayesian change-point linear regression (26) to objectively and quantitatively identify discrete periods of GIA-adjusted sea-level change in North Carolina. We used the GIA-adjusted sea-level data points in this analysis and not the summary polynomial sea-level curve (Figures 2, 3, 4). This

technique is able to provide probabilistic estimates of rates and the timings of rate changes in complex data following many thousands of iterations. Three change-points gave the best fit to the data by providing four successive segments of sea-level change, each of which was described by a linear rate of change. The regression was forced through zero because RSL must equal zero at the time of core collection. The model takes account of calibrated radiocarbon uncertainty by approximating each calibrated age as a normal distribution; it also takes into consideration vertical errors.

This technique provides a most likely sea-level history given the distribution of the data points and the distribution of uncertainties within them. The fitted lines represent mean, long term, sea-level change rates and have 95% upper and lower confidence intervals. The model is necessarily an approximation, as each of the four segments is linear, and changes are instantaneous rather than gradual. For the North Carolina reconstruction, sea level prior to the first change point (AD 853-1076) was between -0.03 and +0.06 mm/yr (95% confidence). From here until the second change point (AD 1274-1476) sea level rose at 0.37-0.80 mm/yr (95% confidence interval). The third segment until a change point at AD 1865-1892 showed sea-level change of -0.16 to +0.02 mm/yr (95% confidence). Since this most recent change point sea level has risen at a rate of 1.90-2.20 mm/yr (95% confidence interval). These ranges represent the uncertainty in fitting a single best fit change point regression through the proxy data. However, due to the age and vertical errors in the proxy sea-level data, shorter-lived sea-level changes (particularly at sub-centennial time scales) exceeding the rates described can be accommodated. Indeed, any sea-level history is permissible with the confines of the error

boxes although the results from change point linear regression suggest that they are less likely than the sea-level changes we described.

Bayesian change point analysis was not applied to the Massachusetts data (or other reconstructions of sea level as presented in Figure 3) because of temporal gaps in the record of up to 400 years. We also calculated a GIA adjusted value of sea-level change during the 20th century from the mid points of AD 1899 (RSL = -0.24 ± 0.04m) and AD 2004 (RSL = 0 ± 0.04m).

Validating sea-level reconstructions using tide-gauge records

Instrumental records of sea-level variability provide a unique opportunity to independently check proxy-based reconstructions. Tide-gauge measurements are commonly averaged to reduce one year of data to a single point. Gauges with more than 50 years of data are considered to be the most representative of sea-level trends as the influence of annual-decadal scale variability is minimized (14, 16, 27). The distribution of such gauges is strongly biased toward the northern hemisphere. The longest tide-gauge records (such as Amsterdam, Liverpool, Brest and Stockholm) are located in northern Europe (28, 29).

Sea-level reconstructions from salt-marshes are developed using 1 cm thick slices of sediment from core material. The effect of this approach is two fold. Firstly, sea-level indicators on salt marshes such as plants and foraminifera do not respond to short-lived variability in sea level. Secondly, the 1 cm slices of sediment represent a period of time,

which is dependent on the rate of sediment accumulation, but is on the order of years. Both of these factors serve to make salt-marshes excellent archives of persistent paleo sea-level trends because short-lived and annual variability is naturally filtered out. Therefore it is unreasonable to expect sea-level reconstructions to resolve sea-level changes with the same resolution as tide gauges. In fact, this filtering means it is often easier to extract sea-level trends from salt marshes than from noisy tide-gauge records.

We consider reconstructed sea level to be in agreement with tide-gauge measurements when persistent trends can be seen in both records and where tide-gauge measurements pass though sea-level reconstruction boxes incorporating age and vertical uncertainties. In Figure 2B we show that tide-gauge data with annual resolution from North Carolina (since AD 1936) and Charleston, South Carolina (since AD 1920) are in agreement with the sea-level reconstructions from Sand Point and Tump Point. Compilations of tide-gauge records with global significance (28, 29) have recently been extended to AD 1700. In figure 3 we show that there is excellent agreement among these records and reconstructed sea level in North Carolina. For the period since AD 1880 the record of Church and White (30) does not leave the summary sea-level envelope constructed for North Carolina and at no point does the mid point of the Jeverejeva et al. record (28) covering the period since AD 1700 leave this envelope (Figure 3). In figure S6 we compare the North Carolina sea-level reconstruction to the global tide gauge-compilation of (28) , where the tide-gauge data was summarized using change point regression. The largest difference between the two datasets was 6 cm which is less than the uncertainty for the North Carolina reconstruction and much of the tide-gauge data. This agreement

provides confidence that salt-marshes in North Carolina provide accurate reconstructions of long term, persistent changes in sea level during the late Holocene.

High-resolution numerical modeling of tidal range change from barrier breaching in the Albemarle–Pamlico estuarine system of North Carolina

If tidal range has changed through time, sea-level reconstructions based upon tide-level indicators will differ from the 'true' sea-level curve. To investigate this influence for Sand Point and Tump Point we modeled the influence of barrier breaching on tidal range using the ADCIRC model. The open boundary of the grid was forced with six tidal constituents and runs were carried out for 60 days of model time, with a 10 day ramp. The final 45 days of the simulations were used to perform a harmonic analysis of the results. This harmonic analysis yielded the amplitudes and phases of 23 tidal constituents. In turn, these constituents were used to determine major tidal datums, such as mean higher high water (MHHW), mean lower low water (MLLW) and so on. Tidal range was taken to be the difference between MHHW and MLLW. The modeled study area covered the Outer Banks area of North Carolina from Bogue Inlet in the south of the domain to the border of North Carolina and Virginia in the north. In this region there are currently six inlets. From north to south these are: Oregon Inlet, Hatteras Inlet and Ocracoke Inlet, which lead into Pamlico Sound; Drum Inlet and Barden Inlet (at Cape Lookout), which lead into Core Sound; Beaufort Inlet and Bogue, which lead into Bogue Sound. The tidal range on the ocean-side of the Outer Banks ranges from about 0.75m to 1.25 m. Once the tide propagates through the northern inlets, it is quickly damped in Pamlico and Albemarle Sounds to a range that is less than 0.25 m and in many places less than 0.15 m.

In Core, Back and Bogue Sounds, tidal range is lower than on the ocean-side of the Outer Banks, but ranges from 0.25 m to 1.1 m.

Small Inlet Breaches

For this study, eight additional inlets were added to the model domain. Each of these new inlets was set to an approximate center depth of 6 m. As with existing inlets, tidal range declined rapidly after the tide propagated through the inlets. Increasing the number of inlets caused tidal range at our study sites to increase on the order of 0.05 m, within the uncertainty band shown for our analysis.

Large Inlet Breaches

To simulate 'catastrophic' collapse of the barrier islands, 6 huge sections of the Outer Banks were removed. The bathymetry that existed in the original grid on either side of the barrier islands was kept, and simply interpolated between these two to create a new depth in the area where the island was supposed to have collapsed. The results from the model simulations show tidal range increases in the sound area. There was significant spatial variability, with larger increases near to Tump Point, and lower increases toward the Pamlico and Neuse River inlets, near the Sand Point site. These differences in tidal range would produce RSL reconstructions from Sand Point and Tump Point that would be different to one another. But the records have near identical sea-level variations. This agreement suggests that tidal-range change was not an important influence on sea level in the region over the past two millennia.

Ice sheet gravity effect on the proxy sea-level data

In addition to the effect of GIA since the last deglaciation, there is also the gravity effect on the geoid of shrinking continental ice sheets, and thus on local sea level. This phenomenon causes local rates of sea-level rise to differ from the global average and has been termed fingerprinting (31). The values found by Mitrovica et al. (31) are provided in Table S2, for two different GIA modeling approaches. The first approach uses, as they explain, “the combination of ice and Earth models adopted in a number of earlier studies”; the second uses a modified GIA model, where lower mantle viscosity is increased from $2x10^{21}$ to $5x10^{21}$ Pa s, in order to better fit historical tide-gauge data along the US Atlantic coast (Table S2).

The "fingerprint" of sea-level rise in North Carolina due to melting of the Greenland Ice Sheet, defined as local sea-level rise expressed as a fraction of global average sea-level rise from this source, is 60% (from Figure 1B in (31)). For small glaciers, the fingerprint is 95% (from Figure 1C in (31)). If we assume a fingerprint of 100% for both Antarctica and “other” (mainly thermosteric rise), we find that the *total* sea-level rise in North Carolina, computed using the above tabulated contributions as weights, is 87% and 83% respectively under the two GIA scenarios (cf. Figure 1A in (31)).

As there is no guarantee that relative contributions from the various continental ice sheets to sea-level rise have been constant over time, it is not feasible to correct the North Carolina record for this effect because the uncertainties are too great. We restrict ourselves here to a sensitivity study, where we assume local sea-level rise to be 83% of

the global average (i.e., we multiply North Carolina sea-level values by 1/0.83 = 1.2) to compare with sea-level curves reconstructed from the temperature proxy data. This exercise is depicted in Figure S2. It is seen that even a worst-case fingerprint effect of 83% leads only to a barely (if at all) visible deterioration of the quality of fit.

Assumed prior information

We assumed the statistics summarized in Table S2 for the reconstructed temperatures, model fit parameters and integration constants.

Bayesian updating to estimate the model parameters

We used Bayes' theorem in the following form:

$$P(\theta|x) = (P(x|\theta) / P(x)\ )\ P(\theta) = L_x(\theta)\ P(\theta),$$

where we defined the likelihood function as

$$L_x(\theta) = \prod_{i=1}^{n} \exp(-\tfrac{1}{2}(H(t_i;\theta)\ H_i)^2 / \sigma^2)\,. \qquad (5)$$

where H_i is a proxy-reconstructed sea-level value, $\theta = \{\tau, a_1, a_2, H_0, \langle T_0 \rangle, T_0(500\text{AD}), T(t)\}$ is the unknown parameter vector for which our Bayesian update will produce a probability density distribution, and $H(t_i; \theta)$ is sea level as predicted from temperature by our relationship for the epoch t_i. Standard error (σ) is the formal uncertainty of the n sea-level proxy data points. H_0 and T_0(AD 500) are integration constants of Eq. (2).

Note that Eq. (5) describes the goodness by which an individual sea-level curve as predicted by our relationship from a Monte-Carlo generated temperature curve "fits through" the observed sea-level points H_i. Thus, in the Bayesian update step this quantity is used to update the *a posteriori* probability of this curve among the generated ensemble. These probabilities, for all ensemble members, are then used to generate *a posteriori* uncertainty bands.

The result of the Bayesian prediction is somewhat dependent on the choice of weighting for the sea-level proxy data; it is necessary to downweight them (or inflate their assumed variance) to take into account that they are subject to strong serial correlation - on which we have no information and which we ignore, as we do the varying precisions of the data points. An appropriate choice for this factor would be 10. With this choice, we find it is not possible to obtain a reasonable *a posteriori* result for the entire data period: it is necessary to exclude the sea-level data before AD 1000 from the fit.

Figure 5 shows the resulting probability density distributions for the unknown parameters and functions of interest, and some correlation point clouds. One sees that parameter a_1 is constrained to 0-0.25 cm/K/yr, and τ to 0-1000 years, with likely values in the 100-500 year range.

Computation and plotting details

We generated the medial curves and uncertainty bands displayed in our plots in the following way. For plots marked *a priori*, we generated 1000 samples, for plots marked *a*

posteriori, 25 000 samples. The plotted curves were smoothed using SSA smoothing (32) with an "embedding dimension" of 15 years, compatible with Vermeer and Rahmstorf (33). A polynomial was fitted to the North Carolina sea-level reconstruction and was used as a visual summary of the data. A 9 degree polynomial (as opposed to one of higher or lower order) was used because it captured the main features of reconstructed sea-level behavior at the timescales we resolve. Raising the degree only marginally improved fit to the data.

Both temperatures and sea levels were plotted relative to a reference level equal to the average for the period AD 1400-1800 (for the Mann et al. (34) reconstructed temperatures and the North Carolina reconstructed sea levels, respectively), corresponding with a reasonable notion of "pre-industrial". In the plots, the reconstructed North Carolina sea levels are represented by a red curve with pink 1σ and 2σ uncertainty bands, cut away for visibility where appropriate.

The values of a_1 and $T_{0,0}$

From the plots in Figure 5 (in particular, the two bottom right ones) it is seen that, while a_1 and $T_{0,0}$ are not separately strongly constrained, nevertheless the product $-a_1 \cdot T_{0,0}$ is constrained, and positive. As a_1 approaches zero from above, $T_{0,0}$ approaches minus infinity. This is a direct consequence of the compatibility condition (35)

$$aT_0 = a_1 T_{0,0} + a_2 \langle T_0 \rangle$$

with the parameters found from the fit to the instrumental period (33). Our results thus suggest a positive value for the secular part of sea-level rise today.

Weighting and fit for the early period (AD 500-1100)

To fit the sea-level proxy data back to AD 500 required down-weighting of the data and generated an inadequate fit with broad uncertainty bands, suggesting that the data is not compatible. Restricting the Bayesian update to only post-AD 1000 sea-level data markedly improved the fit (Figure 3D), but increased divergence between sea-level proxy data and sea level predicted prior to AD 1000. There is independent evidence (21, 22) that the steep sea-level rise predicted from temperatures between AD 500 and 1000 is unphysical, and thus that the sea-level proxy data from North Carolina for this period are more realistic. This is supported by new and published sea-level reconstructions from Massachusetts (SI, (36)) and elsewhere (16, 37).

Lowering reconstructed temperature by 0.2 K for the period AD 500-1100 produced good agreement with the North Carolina sea-level reconstruction (Figure S4). We studied the sensitivity of this fit to a range of temperature corrections (-0.1 K to -0.3 K) as shown in Figure S5, the best agreement was for a -0.2 K correction. An error of this magnitude is not implausible as we used the global Mann et al. (34) reconstruction prior to AD 1100 and not the Northern-Hemisphere-only reconstruction in which (34) had greater confidence. For the period prior to AD 1100, availability of proxy temperature reconstructions is poor for the Southern Hemisphere and this is necessarily reflected in greater uncertainty for global estimates which can accommodate a 0.2 K reduction in temperature within their uncertainty. This reduction in reconstructed temperature would

make the Medieval Climate Anomaly globally less pronounced than Mann et al. (34) suggested, and reduce by a half its temperature contrast with the Little Ice Age.

An alternative explanation is that reconstructed sea level is in error. This does not appear credible because no other sea level reconstruction suggests a stronger sea-level rise before AD 1100 (Figure 3), as warm temperatures would imply under our semi-empirical model. More rapid sea-level rise prior to AD 1100 would be a feature of predicted sea level using the Mann et al. (34) global temperature record and our semi-empirical model regardless of the correction made for GIA. Further, agreement between the Sand Point and Tump Point records, despite differences in accumulation history and being more than 100 km apart suggests that local-scale factors were not important influences on RSL.

While the Grinsted et al. (38) prediction of former sea level is somewhat similar to ours, it features large sea-level variations (greater than 0.5 m) during the last 2000 years (see Figure S6). The magnitude of these predicted sea-level changes is dependent on the temperature reconstructions used as input and their uncertainties. Only for the post- AD 1700 period, for which (38) used tide-gauge data from northwestern Europe to calibrate their model, is there a good agreement with our result. This agreement implies that these extended tide-gauge records are representative of former sea level.

Performance over the instrumental period

We tested the performance of our relationship over the instrumental period, AD 1880-2000 (Figure 6). For temperatures, taken from Mann et al. (34), this is essentially a

test of HadCRUTv3. For instrumental sea level, we took Church and White (29), with an estimated contribution due to the artificial reservoir effect added as described in (33).

Loose parameter constraints

We also produced a reconstruction in which we did not use the prior constraints on the parameters from (33). Instead, we used the following, loose constraints, effectively producing near-ignorant priors:

a = 0.44 ±0.5 cm/K/yr

b = 0 (exactly)

T_0 (AD 1880-2000) = -0.45 ±0.3 K

Furthermore we loosened the constraint of the integration constant H_0 to be U(-10 cm, 10 cm). The reason for fixing b was, that it is not possible to simultaneously solve for a and b using only the paleo data, as we found this to be an ill-posed problem. Fixing b to another value will only change the value obtained for a and not produce any other significant changes to the solution.

For this run we used a sample size of 250 000 instead of the usual 25 000. We found the following posteriors:

a = 0.60 ±0.15 cm/K/yr

$-a_1 \bullet T_{0,0}$ = 0.139 ±0.043 cm/yr

$\ln(\tau) = 5.83 \pm 0.78$ [τ in years]

From Figure S3 we see that τ is still robustly constrained to be finite. Also, remarkably, $-a_1 \bullet T_{0,0}$, a measure for long-term (inter-millennial) sea-level rise, is seen to be very likely positive. And note that coefficient *a* is resolved to a value even larger than is typically obtained from semi-empirical fits to the instrumental period.

The reason for the somewhat larger *a* is that the 20th century rise in the North Carolina data is somewhat larger than that given by global sea-level reconstructions from instrumental data, as discussed in the paper. That is why our preferred modeled sea level curve (Figure 4D) was constrained with instrumental data after AD 1880. Also the fingerprint effect should be considered, correcting for which however would tend to make *a* larger still.

Supporting References

1. Kemp AC, Horton BP, & Culver SJ (2009) Distribution of modern salt-marsh foraminifera in the Albemarle-Pamlico estuarine system of North Carolina, USA: Implications for sea-level research. *Marine Micropaleontology* 72(3-4):222-238.
2. Kemp AC, *et al.* (2009) Timing and magnitude of recent accelerated sea-level rise (North Carolina, United States). *Geology* 37(11):1035-1038.
3. Edwards RJ (2007) Sea Level Studies: Low energy coasts sedimentary indicators. *Encyclopedia of Quaternary Science*, ed Elias SA (Elsevier, Amsterdam), pp 2994-3005.
4. Birks HJB (1995) Quantitative palaeoenvironmental reconstructions. *Statistical Modelling of Quaternary Science Data*, Technical Guide, eds Maddy D & Brew JS (Quaternary Research Association, Cambridge), Vol Technical Guide 5, pp 161-254.
5. Donnelly JP, Cleary P, Newby P, & Ettinger R (2004) Coupling instrumental and geological records of sea-level change: evidence from southern New England of an increase in the rate of sea-level rise in the late 19th century. *Geophysical Research Letters* 31(5):L05203.
6. Appleby PG & Oldfield F (1992) Application of Lead-210 to Sedimentation Studies. *Uranium Series Disequilibrium: Applications to Environmental Problems*, eds Ivanovich M & Harmon RS (Clarendon Press), pp 731-778.
7. Reimer PJ, *et al.* (2004) IntCal04 terrestrial radiocarbon age calibration, 0-26 cal kyr BP. *Radiocarbon* 46(3):1029-1058.
8. Marshall WA, *et al.* (2007) The use of 'bomb spike' calibration and high-precision AMS C-14 analyses to date salt-marsh sediments deposited during the past three centuries. (Translated from English) *Quaternary Research* 68(3):325-337 (in English).
9. Cooper S, McGlothlin S, Madritch M, & Jones D (2004) Paleoecological evidence of human impacts on the Neuse and Pamlico estuaries of North Carolina, USA. *Estuaries and Coasts* 27(4):617-633.
10. Parnell AC, Haslett J, Allen JRM, Buck CE, & Huntley B (2008) A flexible approach to assessing synchroneity of past events using Bayesian reconstructions of sedimentation history. *Quaternary Science Reviews* 27(19-20):1872-1885.
11. Milne GA, Long AJ, & Bassett SE (2005) Modelling Holocene relative sea-level observations from the Caribbean and South America. *Quaternary Science Reviews* 24(10-11):1183.
12. Peltier WR (1996) Global sea level rise and glacial isostatic adjustment: an analysis of data from the east coast of North America. *Geophysical Research Letters* 23:GL00848.
13. Peltier WR (2002) On eustatic sea level history: Last Glacial Maximum to Holocene. *Quaternary Science Reviews* 21(1-3):377.
14. Douglas BC (1995) Global sea level change: Determination and interpretation. *Reviews of Geophysics* 33:1425-1432.
15. Horton BP, *et al.* (2009) Holocene sea-level changes along the North Carolina Coastline and their implications for glacial isostatic adjustment models. *Quaternary Science Reviews* 28(17-18):1725-1736.

16. Engelhart SE, Horton BP, Douglas BC, Peltier WR, & Tornqvist TE (2009) Spatial variability of late Holocene and 20th century sea-level rise along the Atlantic coast of the United States. *Geology* 37(12):1115-1118.
17. Gehrels WR, Belknap DF, Black S, & Newnham RM (2002) Rapid sea-level rise in the Gulf of Maine, USA, since AD 1800. *The Holocene* 12(4):383-389.
18. Gehrels WR, *et al.* (2005) Onset of recent rapid sea-level rise in the western Atlantic Ocean. *Quaternary Science Reviews* 24(18-19):2083-2100.
19. González JL & Törnqvist TE (2009) A new Late Holocene sea-level record from the Mississippi Delta: evidence for a climate/sea level connection? *Quaternary Science Reviews* 28(17-18):1737-1749.
20. Gehrels WR, *et al.* (2006) Rapid sea-level rise in the North Atlantic Ocean since the first half of the nineteenth century. *Holocene* 16(7):949-965.
21. Sivan D, *et al.* (2004) Ancient coastal wells of Caesarea Maritima, Israel, an indicator for relative sea level changes during the last 2000 years. *Earth and Planetary Science Letters* 222(1):315-330.
22. Lambeck K, Anzidei M, Antonioli F, Benini A, & Esposito A (2004) Sea level in Roman time in the Central Mediterranean and implications for recent change. *Earth and Planetary Science Letters* 224(3-4):563-575.
23. Goodwin ID & Harvey N (2008) Subtropical sea-level history from coral microatolls in the Southern Cook Islands, since 300 AD. *Marine Geology* 253(1-2):14-25.
24. Peltier WR (2001) Global glacio isostatic adjustment and modern instrument records of relative sea level history. *Sea-level rise history and consequences*, eds Douglas BC, Kearney MS, & Leatherman SP (Academic Press, San Diego).
25. van de Plassche O, van der Borg K, & de Jong AFM (1998) Sea level-climate correlation during the past 1400 yr. *Geology* 26(4):319-322.
26. Carlin BP, Gelfand AE, & Smith AFM (1992) Hierarchical Bayesian Analysis of Changepoint Problems. *Applied Statistics* 41(2):389-405.
27. Douglas BC (1991) Global Sea Level Rise. *Journal of Geophysical Research* 96(C4):6981-6992.
28. Jevrejeva S, Moore JC, Grinsted A, & Woodworth PL (2008) Recent global sea level acceleration started over 200 years ago? *Geophysical Research Letters* 35(8):L08715.
29. Church JA & White NJ (2006) A 20th century acceleration in global sea-level rise. *Geophysical Research Letters* 33(1):L01602.
30. Church J, *et al.* (2008) Understanding global sea levels: past, present and future. *Sustainability Science* 3(1):9.
31. Mitrovica JX, Tamisiea ME, Davis JL, & Milne GA (2001) Recent mass balance of polar ice sheets inferred from patterns of global sea-level change. *Nature* 409(6823):1026-1029.
32. Moore JC, Grinsted A, & Jevrejeva S (2005) The new tools for analyzing the time series relationships and trends. *Eos Trans. AGU* 86(24):226.
33. Vermeer M & Rahmstorf S (2009) Global sea level linked to global temperature. *Proceedings of the National Academy of Sciences* 106(51):21527-21532.

34. Mann ME, *et al.* (2008) Proxy-based reconstructions of hemispheric and global surface temperature variations over the past two millennia. *Proceedings of the National Academy of Sciences* 105(36):13252-13257.
35. Rahmstorf S (2007) A Semi-Empirical Approach to Projecting Future Sea-Level Rise. *Science* 315(5810):368-370.
36. Donnelly JP (2006) A revised late Holocene sea-level record for northern Massachusetts, USA. (Translated from English) *Journal of Coastal Research* 22(5):1051-1061 (in English).
37. Peltier WR (2001) Global sea level rise and glacial isostatic adjustment: an analysis of data from the east coast of North America. *Geophysical Research Letters* 23.
38. Grinsted A, Moore J, & Jevrejeva S (2009) Reconstructing sea level from paleo and projected temperatures 200 to 2100 ad. *Climate Dynamics*:doi: 10.1007/s00382-00008-00507-00382.
39. Moberg A, Sonechkin DM, Holmgren K, Datsenko NM, & Karlen W (2005) Highly variable Northern Hemisphere temperatures reconstructed from low- and high-resolution proxy data. *Nature* 433(7026):613-617.
40. Jones PD & Mann ME (2004) Climate over past millennia. *Reviews of Geophysics* 42:2003RG000143.
41. Brohan P, Kennedy JJ, Harris I, Tett SFB, & Jones PD (2006) Uncertainty estimates in regional and global observed temperature changes: a new dataset from 1850. *Journal of Geophysical Research* 111(D12):D12106.

Supporting Figure Captions

Figure S1: Chronostratigraphy of the Wood Island (Massachusetts) site developed using AMS ^{14}C dating, heavy metal concentrations (Cu and Pb), opaque spherules (O-S) and pollen. Metal concentrations are presented as integrated peak area (ints), opaque sperhule abundance is expressed as a percentage of total pollen ($\%_{tp}$). PME was estimated using plant macrofossils (Jg = *Juncus geradii*; Sp/Ds = *Spartina patens* or *Distichlis spicata*). The modern distribution of these plants with respect to sea level was estimated by repeated leveling at the Wood Island site. Samples were collected from the sediment-erratic contact exposed by excavating a trench and are presented as depth below modern marsh surface. Chronological horizons are shown by grey shading.

Figure S2: Sensitivity analysis for the ice sheet gravity effect in North Carolina. (A) Sea-level reconstruction from paleo-temperature (grey) and proxy-reconstructed sea levels from North Carolina with uncertainties as cutaway color bands (pink). Scaled for a North Carolina fingerprint of 83% of global sea-level rise. GIA-adjusted sea level is expressed relative to AD 1400-1800 average. (B) Posterior probability density distributions and correlation point clouds for selected quantities; ka is thousand years.

Figure S3: Sea level reconstruction (grey) for relaxed prior constraints on the parameters a, b, $<T_0$(AD1880-2000)> and H_0, with histograms and scatter plots as insets. Proxy-reconstructed sea levels from North Carolina with uncertainties as cutaway color bands in pink. GIA-adjusted sea level is expressed relative to AD 1400-1800 average.

Figure S4: Sea-level predicted from paleo-temperature data, using sea-level proxy data from the whole period. Shaded error bands indicate 1σ and 2σ uncertainties. A correction of -0.2 K was applied to temperatures for AD 500-1100. (**A**) Temperature expressed relative to AD 1400-1800 average (grey; original from (34) = red, reconstructed; median = black) and equilibrium temperature (blue). (**B**) Sea level predicted from adjusted temperature (grey) and summary of proxy-reconstructed sea levels from North Carolina (pink). GIA-adjusted sea level expressed relative to AD 1400-1800 average.

Figure S5: The effect of amending reconstructed temperature for the period before AD 1100. Adjustments of (A) 0.0 K; (B) -0.1 K; (C) -0.2 K; and (D) -0.3 K were made to the composite error-in-variables land plus ocean global temperature reconstruction of (34). Proxy-reconstructed sea levels from North Carolina with uncertainties as cutaway color bands (pink). GIA-adjusted sea level is expressed relative to AD 1400-1800 averages. Sea level is in comparison to the average for AD 1400-1800 and has been adjusted for glacio-isostatic adjustment.

Figure S6: (A) Comparison of reconstructed sea level from North Carolina (pink) and sea-level hindcasts from the semi-empirical model of Grinsted et al. (38). Two reconstructions of climate (39, 40) were used to predict former sea level from the semi-empirical model of Grinsted et al. (38). Uncertainties in sea-level hindcasts are not presented. Predictions using the Moberg dataset (39) were favored by (38). Sea level for each dataset is adjusted for GIA and expressed relative to AD 1400-1800 average.

(B) Comparison of GIA-adjusted sea-level reconstruction from North Carolina (red, with pink error bounds) with the global tide-gauge compilation (grey with error bounds) of (28). The tide-gauge data were summarized using change point regression (blue, with 95% confidence interval). All series are shown relative to the average over the period AD 1950-2000.

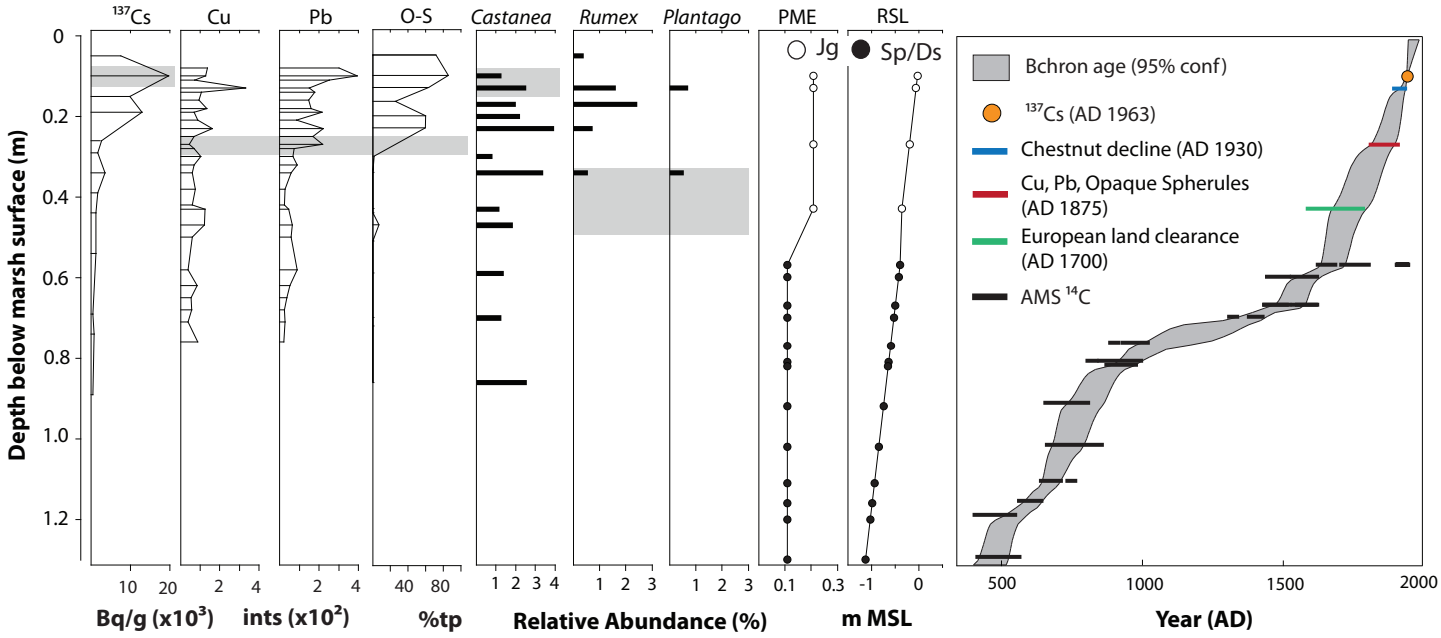
137Cs
Cu
Pb
O-S
Castanea
Rumex
Plantago
PME
RSL
Jg
Sp/Ds
Depth below marsh surface (m)
0
0.2
0.4
0.6
0.8
1.0
1.2
10 20
2 4
2 4
40 80
1 2 3 4
1 2 3
1 2 3
0.1 0.3
-1 0
Bq/g (x10³)
ints (x10²)
%tp
Relative Abundance (%)
m MSL
Bchron age (95% conf)
137Cs (AD 1963)
Chestnut decline (AD 1930)
Cu, Pb, Opaque Spherules (AD 1875)
European land clearance (AD 1700)
AMS 14C
500
1000
1500
2000
Year (AD)

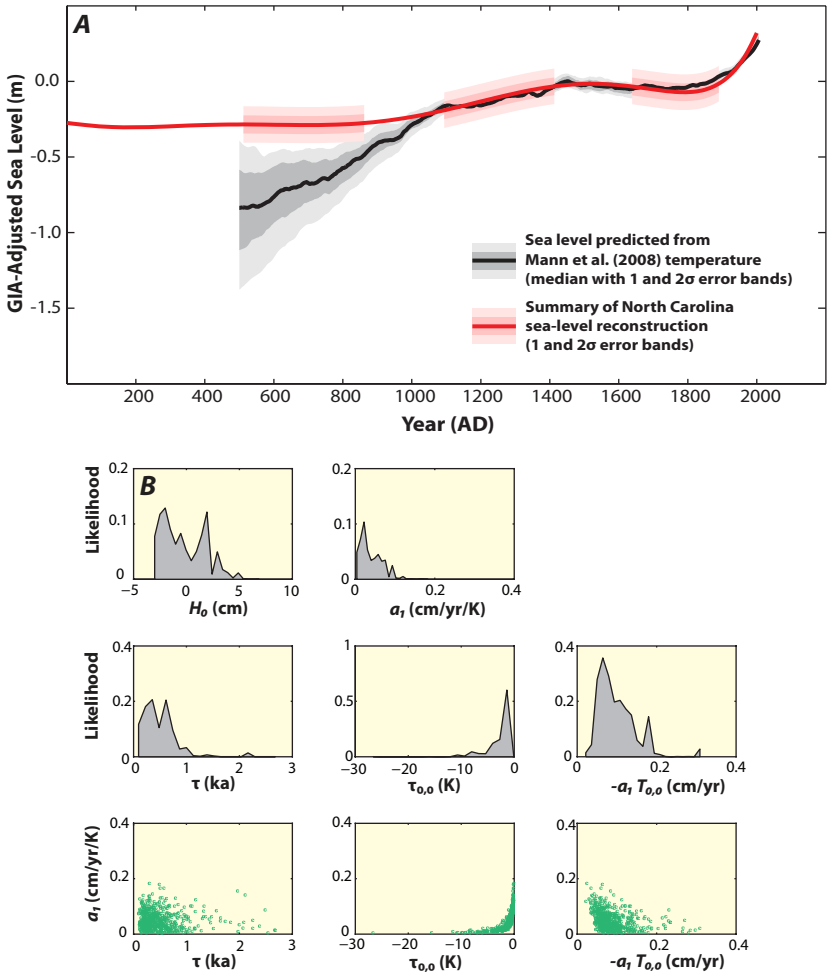
A
GIA-Adjusted Sea Level (m)
0.0
-0.5
-1.0
-1.5
200
400
600
800
1000
1200
1400
1600
1800
2000
Year (AD)
Sea level predicted from
Mann et al. (2008) temperature
(median with 1 and 2σ error bands)
Summary of North Carolina
sea-level reconstruction
(1 and 2σ error bands)
B
Likelihood
H_o (cm)
a_1 (cm/yr/K)
τ (ka)
$\tau_{o,o}$ (K)
$-a_1 T_{o,o}$ (cm/yr)

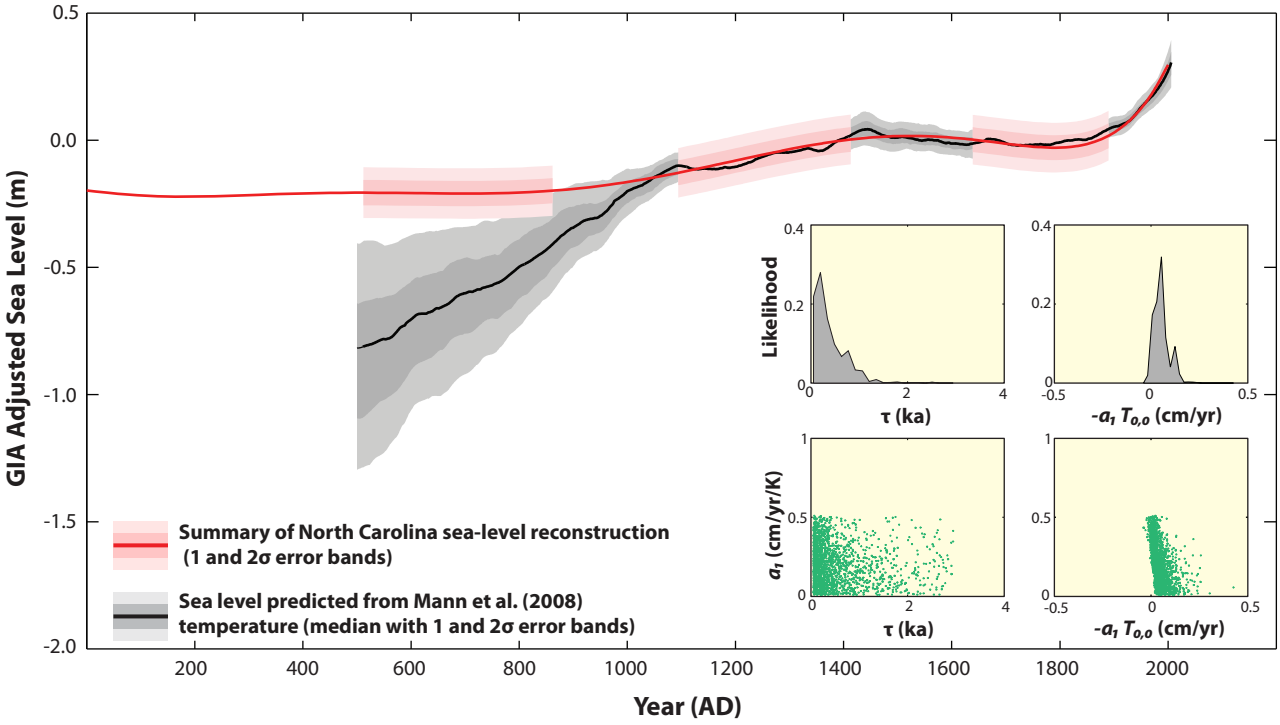
GIA Adjusted Sea Level (m)
0.5
0.0
-0.5
-1.0
-1.5
-2.0
200
400
600
800
1000
1200
1400
1600
1800
2000
Year (AD)
Summary of North Carolina sea-level reconstruction
(1 and 2σ error bands)
Sea level predicted from Mann et al. (2008)
temperature (median with 1 and 2σ error bands)
Likelihood
τ (ka)
-a1 T0,0 (cm/yr)
a1 (cm/yr/K)

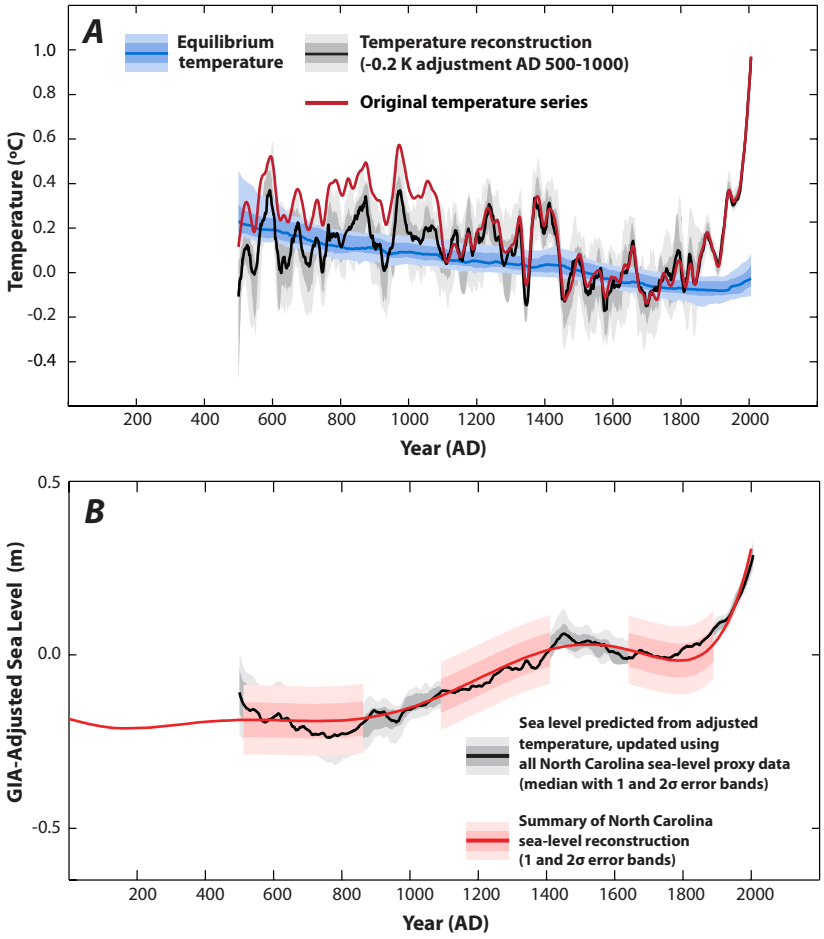
A
Equilibrium temperature
Temperature reconstruction (-0.2 K adjustment AD 500-1000)
Original temperature series
Temperature (°C)
1.0
0.8
0.6
0.4
0.2
0.0
-0.2
-0.4
200
400
600
800
1000
1200
1400
1600
1800
2000
Year (AD)
B
GIA-Adjusted Sea Level (m)
0.5
0.0
-0.5
Sea level predicted from adjusted temperature, updated using all North Carolina sea-level proxy data (median with 1 and 2σ error bands)
Summary of North Carolina sea-level reconstruction (1 and 2σ error bands)
200
400
600
800
1000
1200
1400
1600
1800
2000
Year (AD)

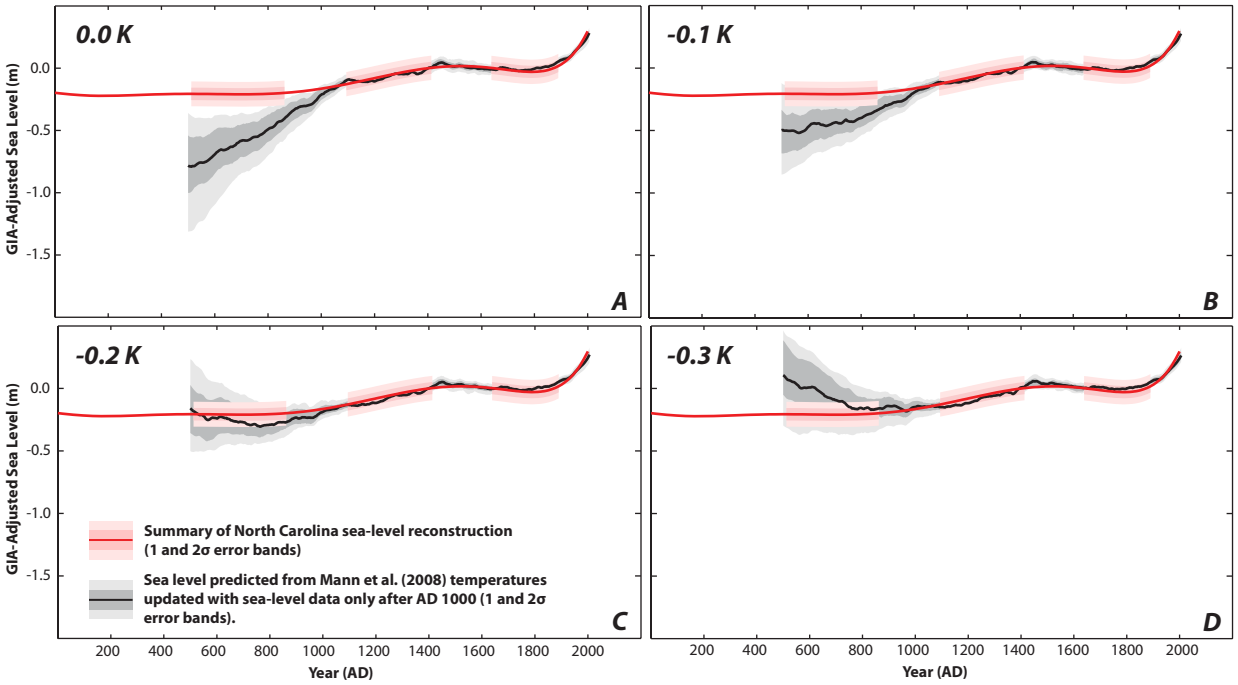
0.0 K
-0.1 K
-0.2 K
-0.3 K
A
B
C
D
GIA-Adjusted Sea Level (m)
0.0
-0.5
-1.0
-1.5
200
400
600
800
1000
1200
1400
1600
1800
2000
Year (AD)
Summary of North Carolina sea-level reconstruction (1 and 2σ error bands)
Sea level predicted from Mann et al. (2008) temperatures updated with sea-level data only after AD 1000 (1 and 2σ error bands).

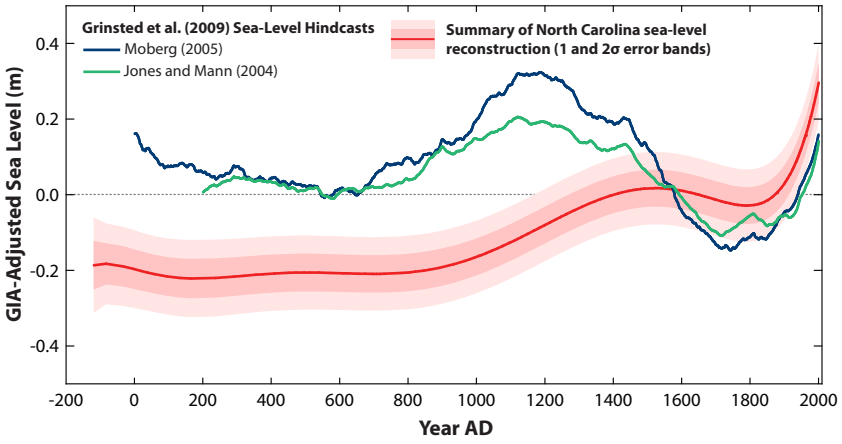
Grinsted et al. (2009) Sea-Level Hindcasts
Moberg (2005)
Jones and Mann (2004)
Summary of North Carolina sea-level reconstruction (1 and 2σ error bands)
GIA-Adjusted Sea Level (m)
0.4
0.2
0.0
-0.2
-0.4
-200
0
200
400
600
800
1000
1200
1400
1600
1800
2000
Year AD

Table S1: Sea-level data points from North Carolina (Sand Point = SP and Tump Point = TP) and Wood Island Massachusetts. RSL = relative sea level.

North Carolina

Year (AD/BC)	RSL (m)	Age Error (yrs)	RSL Error (m)	Site
2000	0.02	2	0.03	TP
1995	0.02	1	0.04	TP
1986	0.00	5	0.03	TP
1977	-0.01	4	0.03	TP
1977	-0.07	3	0.05	SP
1973	0.00	4	0.03	TP
1973	-0.11	3	0.05	SP
1969	-0.10	2	0.05	SP
1965	-0.16	2	0.05	SP
1961	-0.07	3	0.03	TP
1961	-0.18	2	0.05	SP
1959	-0.17	2	0.05	SP
1959	-0.07	2	0.03	TP
1957	-0.17	2	0.05	SP
1956	-0.08	2	0.03	TP
1948	-0.19	3	0.05	SP
1946	-0.16	5	0.03	TP
1944	-0.25	3	0.05	SP
1942	-0.17	3	0.09	SP
1940	-0.17	3	0.08	SP
1939	-0.18	5	0.03	TP
1938	-0.21	4	0.06	SP
1937	-0.22	4	0.07	SP
1935	-0.19	4	0.04	SP
1935	-0.15	5	0.03	TP
1934	-0.27	4	0.06	SP
1933	-0.23	5	0.05	SP
1931	-0.25	5	0.05	SP
1927	-0.21	6	0.03	TP
1926	-0.31	5	0.05	SP
1924	-0.24	6	0.03	TP
1922	-0.32	5	0.05	SP
1916	-0.26	6	0.03	TP
1915	-0.30	5	0.06	SP
1909	-0.31	7	0.04	TP
1909	-0.28	5	0.07	SP
1904	-0.32	6	0.06	SP
1903	-0.32	7	0.04	TP
1900	-0.34	8	0.04	TP
1890	-0.38	8	0.04	TP
1877	-0.35	22	0.05	SP
1877	-0.39	14	0.04	TP

1865	-0.40	18	0.03	TP
1852	-0.40	19	0.03	TP
1849	-0.39	35	0.06	SP
1840	-0.39	35	0.06	SP
1833	-0.46	18	0.04	TP
1831	-0.41	33	0.05	SP
1826	-0.46	16	0.03	TP
1822	-0.41	30	0.07	SP
1811	-0.42	25	0.06	SP
1793	-0.45	20	0.06	SP
1785	-0.43	21	0.03	TP
1777	-0.44	18	0.06	SP
1764	-0.47	24	0.06	SP
1760	-0.48	29	0.03	TP
1751	-0.50	27	0.05	SP
1739	-0.47	26	0.07	SP
1727	-0.54	33	0.03	TP
1726	-0.52	21	0.05	SP
1715	-0.53	33	0.03	TP
1697	-0.56	29	0.06	SP
1692	-0.56	29	0.03	TP
1676	-0.57	36	0.04	SP
1667	-0.57	26	0.03	TP
1657	-0.58	40	0.04	SP
1650	-0.62	28	0.03	TP
1648	-0.59	40	0.04	SP
1641	-0.63	29	0.03	TP
1639	-0.59	40	0.05	SP
1629	-0.63	38	0.06	SP
1623	-0.64	28	0.03	TP
1604	-0.56	27	0.03	TP
1591	-0.59	27	0.03	TP
1590	-0.66	34	0.06	SP
1575	-0.65	37	0.05	SP
1571	-0.63	32	0.03	TP
1559	-0.72	38	0.05	SP
1542	-0.66	35	0.03	TP
1522	-0.65	34	0.03	TP
1515	-0.72	41	0.05	SP
1490	-0.67	30	0.03	TP
1488	-0.73	43	0.07	SP
1479	-0.74	42	0.05	SP
1467	-0.71	30	0.03	TP
1461	-0.76	39	0.06	SP
1447	-0.73	28	0.03	TP
1443	-0.78	32	0.06	SP
1416	-0.81	24	0.05	SP
1413	-0.82	25	0.03	TP
1392	-0.82	30	0.05	SP
1388	-0.84	34	0.03	TP

1362	-0.84	40	0.03	TP
1360	-0.87	38	0.06	SP
1345	-0.88	42	0.03	TP
1331	-0.93	37	0.05	SP
1307	-0.93	28	0.06	SP
1286	-0.97	46	0.03	TP
1284	-1.01	19	0.06	SP
1262	-0.99	22	0.05	SP
1261	-0.96	46	0.03	TP
1246	-1.03	26	0.06	SP
1243	-0.97	46	0.03	TP
1231	-1.04	30	0.05	SP
1215	-1.00	46	0.03	TP
1213	-1.11	35	0.06	SP
1200	-1.01	52	0.03	TP
1196	-1.14	38	0.05	SP
1184	-1.15	39	0.05	SP
1180	-1.05	59	0.03	TP
1167	-1.08	63	0.03	TP
1167	-1.15	39	0.06	SP
1152	-1.20	40	0.05	SP
1148	-1.08	68	0.03	TP
1131	-1.21	76	0.04	TP
1131	-1.23	40	0.06	SP
1119	-1.26	41	0.06	SP
1110	-1.23	96	0.03	TP
1097	-1.22	107	0.03	TP
1094	-1.29	40	0.05	SP
1077	-1.26	125	0.03	TP
1075	-1.32	40	0.06	SP
1058	-1.34	38	0.05	SP
1044	-1.23	153	0.03	TP
1040	-1.36	35	0.05	SP
1029	-1.39	32	0.05	SP
1025	-1.30	168	0.03	TP
1012	-1.30	179	0.03	TP
1006	-1.40	27	0.05	SP
992	-1.33	193	0.03	TP
979	-1.44	36	0.06	SP
966	-1.46	39	0.05	SP
932	-1.52	41	0.05	SP
889	-1.54	52	0.05	SP
862	-1.58	57	0.06	SP
845	-1.58	59	0.06	SP
821	-1.62	59	0.06	SP
804	-1.62	60	0.05	SP
780	-1.66	58	0.05	SP
729	-1.72	56	0.06	SP
717	-1.73	58	0.06	SP
707	-1.70	60	0.04	SP

696	-1.71	61	0.04	SP
674	-1.76	62	0.04	SP
653	-1.85	61	0.04	SP
620	-1.89	56	0.05	SP
611	-1.87	54	0.05	SP
572	-1.91	46	0.06	SP
538	-1.86	50	0.06	SP
512	-1.96	52	0.04	SP
495	-1.94	52	0.05	SP
471	-1.98	48	0.06	SP
450	-2.05	48	0.07	SP
407	-2.02	56	0.05	SP
375	-2.14	59	0.05	SP
354	-2.06	59	0.05	SP
318	-2.16	58	0.05	SP
290	-2.19	62	0.05	SP
237	-2.22	68	0.06	SP
164	-2.28	69	0.05	SP
132	-2.28	65	0.06	SP
94	-2.41	60	0.06	SP
57	-2.42	63	0.06	SP
37	-2.42	65	0.09	SP
17	-2.42	67	0.07	SP
-3	-2.42	69	0.05	SP
-33	-2.50	68	0.06	SP
-84	-2.51	63	0.08	SP
-120	-2.55	59	0.08	SP

Massachusetts

Year (AD)	RSL (m)	Age Error (yrs)	RSL Error (m)
1963	-0.02	0	0.11
1930	-0.05	10	0.11
1875	-0.19	25	0.11
1700	-0.35	50	0.11
1669	-0.39	25	0.11
1600	-0.42	90	0.11
1487	-0.49	95	0.11
1486	-0.49	91	0.11
1415	-0.52	60	0.11
997	-0.59	68	0.11
941	-0.63	54	0.11
932	-0.64	100	0.11
728	-0.74	101	0.11
707	-0.84	96	0.11
671	-0.93	61	0.11
619	-0.98	40	0.11
507	-1.02	74	0.11
463	-1.12	78	0.11

Table S2: Fingerprints for North Carolina and other areas with proxy sea-level data

	Greenland (mm/yr)	**Antarctica plus others (mm/yr)**	**Meier (mm/yr)**	**Sum (mm/yr)**			
Wt (1)	0.54	0.99	0.46	1.99			
Wt (2)	0.60	0.61	0.46	1.67		Factors relative to NC	
				For wt (1)	For wt (2)	x NC (1)	x NC (2)
Nova Scotia	0.20	1.00	0.90	0.76	0.69	1.14	1.21
Massachusetts	0.30	1.00	0.90	0.79	0.72	1.10	1.15
Connecticut	0.40	1.00	0.90	0.81	0.76	1.07	1.09
North Carolina	0.60	1.00	0.90	0.87	0.83	1.00	1.00
Louisiana	0.80	1.00	0.95	0.93	0.91	0.93	0.91

Wt (1) uses ice and Earth models (32)
Wt (2) uses a modified GIA model, where lower mantle viscosity is increased from $2x10^{21}$ to $5x10^{21}$ Pa s, in order to better fit to tide gauges on the US Atlantic coast (32)

Table S3: Assumed prior statistics. $M(t)$ refers to the proxy-reconstructed paleo-temperatures used; C is a constant chosen for computational reasons such that the prior will not constrain the posterior. $N(\mu, \sigma^2)$ is the normal distribution of central value μ and variance σ^2; $U(a,b)$ is the uniform distribution between a and b. K is Kelvin.

Item	**Distribution**	**Remarks**
$T(t <$AD 1850)	$M(t)+N(0, (0.15\ \mathrm{K})^2)$	decadal, uncorrelated; (35)
T(AD 1850-1950)	$M(t)+N(0, (0.06\ \mathrm{K})^2)$	decadal, uncorrelated; (42)
T(AD 1950-2006)	$M(t)+N(0, (0.04\ \mathrm{K})^2)$	decadal, uncorrelated; (42)
a	$N(0.56\ \mathrm{cm/yr/K}, (0.05\ \mathrm{cm/yr/K})^2)$	(34)
$<T_0$(AD1880-2000)>	$<T$(AD 1951-1980)> $+N(-0.41\ \mathrm{K}, (0.03\ \mathrm{K})^2)$	(34) constrained T_0 for this interval
a_1	$U(0.01,0.51)$ cm/yr/K	secular response part
b	$N(-4.9\ \mathrm{cm/K}, (1.0\ \mathrm{cm/K})^2)$	(34)
τ	$400 \bullet \exp(U(-2,2))$ yrs	$\ln(\tau)$ uniformly distributed for τ=135-7400 years
T_0(AD500)	$N(<T$(AD 500-700)>, $(0.2\ \mathrm{K})^2)$	starting value for T_0 integration
H_0	$C+U(-5,5)$ cm	sea-level integration constant